AD-A143 183 DEVELOPMENT OF AN X-RAY FACILITY FOR RADIATION DOSIMETRY STUDIES(U) MATERIALS RESEARCH LABS ASCOT VALE (AUSTRALIA) R B HUNTLEY DEC 83 MRL-R-910 1/ 1

UNCLASSIFIED F/G 6/18 NL

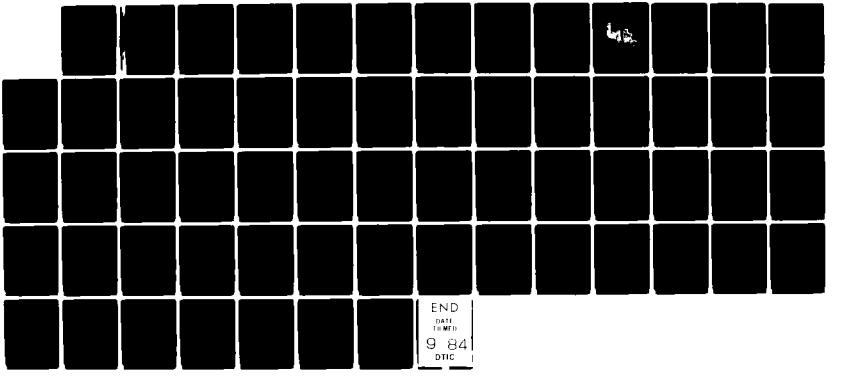

END
DATE FILMED
9 84
DTIC

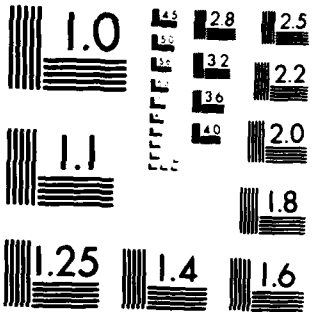

MRL-R-910

AR-003-807

DEPARTMENT OF DEFENCE

DEFENCE SCIENCE AND TECHNOLOGY ORGANISATION

MATERIALS RESEARCH LABORATORIES

MELBOURNE, VICTORIA

REPORT

MRL-R-910

DEVELOPMENT OF AN X-RAY FACILITY FOR RADIATION DOSIMETRY STUDIES

R.B. Huntley*

Approved for Public Release

* Present address: Australian Radiation Laboratory
Commonwealth Department of Health
Lower Plenty Road
YALLAMBIE VIC 3085

DECEMBER, 1983

DEPARTMENT OF DEFENCE

MATERIALS RESEARCH LABORATORIES

REPORT

MRL-R-910

DEVELOPMENT OF AN X-RAY FACILITY FOR RADIATION DOSIMETRY STUDIES

R.B. Huntley*

ABSTRACT

An X-ray test facility is described which provides photon beams of sharply-defined energy in the range 5 to 250 keV. Methods adopted include the use of composite filters and radiator foils. Characteristics of the radiation beams are established, including their intensities, energy spectra, and transverse uniformities, and a novel operating chart is presented. The facility may be employed for a wide range of radiation experiments, and its application to the testing and calibration of civilian, military, and civil defence radiation measuring instruments is considered in detail.

Approved for Public Release

*Present address: Australian Radiation Laboratory
Commonwealth Department of Health
Lower Plenty Road,
YALLAMBIE, VIC 3085

SECURITY CLASSIFICATION OF THIS PAGE UNCLASSIFIED

DOCUMENT CONTROL DATA SHEET

REPORT NO.	AR NO.	REPORT SECURITY CLASSIFICATION
MRL-R-910	AR-003-807	UNCLASSIFIED

TITLE

DEVELOPMENT OF AN X-RAY FACILITY FOR RADIATION DOSIMETRY STUDIES

AUTHOR(S)

HUNTLEY, R.B.

CORPORATE AUTHOR
Materials Research Laboratories
P.O. Box 50,
Ascot Vale, Victoria 3032

REPORT DATE	TASK NO.	SPONSOR
DECEMBER, 1983	DST 78/034	DSTO

CLASSIFICATION/LIMITATION REVIEW DATE	CLASSIFICATION/RELEASE AUTHORITY
---	Superintendent, MRL Physics Division

SECONDARY DISTRIBUTION

Approved for Public Release

ANNOUNCEMENT

Announcement of this report is unlimited

KEYWORDS

X-RAY APPARATUS
DOSIMETRY
FILTERS
CALIBRATION

COSATI GROUPS 1306

ABSTRACT

An X-ray test facility is described which provides photon beams of sharply-defined energy in the range 5 to 250 keV. Methods adopted include the use of composite filters and radiator foils. Characteristics of the radiation beams are established, including their intensities, energy spectra, and transverse uniformities, and a novel operating chart is presented. The facility may be employed for a wide range of radiation experiments, and its application to the testing and calibration of civilian, military, and civil defence radiation measuring instruments is considered in detail.

CONTENTS

CONTENTS

(Continued)

TABLES

FIGURES

FIGURES

(Continued)

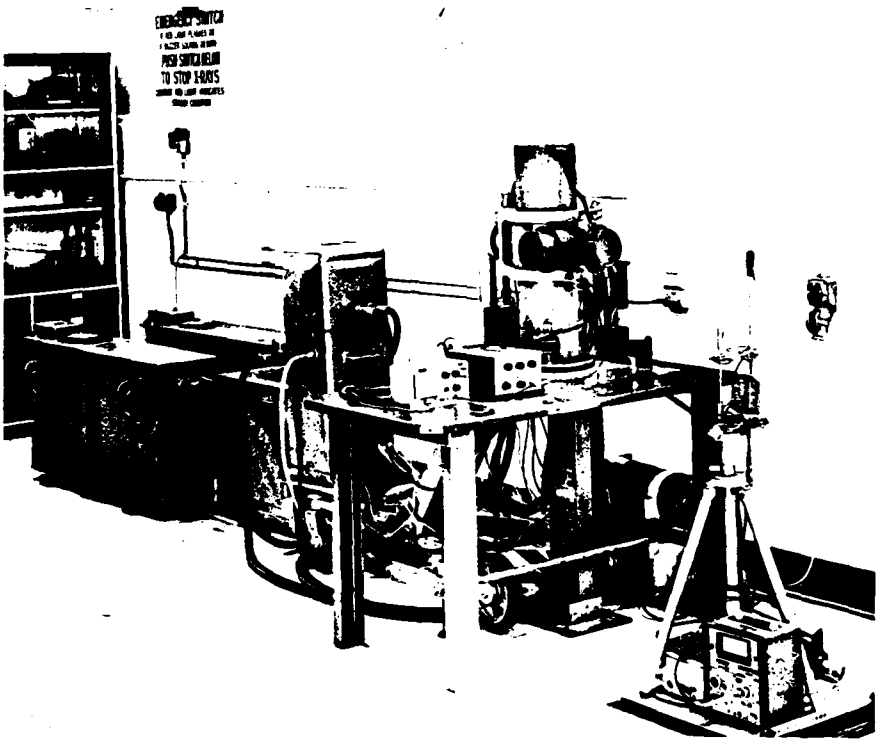

300 kV Constant Potential X-ray Generator

DEVELOPMENT OF AN X-RAY FACILITY FOR RADIATION DOSIMETRY STUDIES

1. INTRODUCTION

Experimental work in an ionising radiation physics laboratory requires well-characterised sources of ionising radiation. This report describes an X-ray test facility, which can be used to provide a radiation beam of any effective photon energy in the range 5 to 250 keV. It is not feasible to use radioactive sources for this purpose, as few emit low energy photons with useful intensity, and those that do are short-lived or expensive. Radioactive sources are useful for higher photon energies, and the X-ray facility is supplemented in this laboratory by test facilities of this type; for example, by using caesium-137 and cobalt-60 sources, photon energies of about 0.66 and 1.25 MeV, respectively, may be obtained.

Fig. 1 shows the photon energies of the test facilities compared with the energy ranges of typical radiation measuring equipment. Whereas civilian radiation protection instruments may be required to measure photons with energies from 5 keV upwards, military and civil defence instruments (called RADIAC instruments) must measure photons in the energy range 80 keV to several MeV, with the response falling off sharply below 80 keV. It can be seen that the X-ray facility covers an important part of the photon energy range and, in conjunction with other facilities, enables the energy response characteristics of radiation measuring instruments to be tested. This application of the facility is especially important in connection with research into new methods of radiation measurement, and the development of improved instruments. Instruments with a range of sensitivities may be tested, as a wide range of intensities is available at any effective photon energy.

The X-ray facility is suitable for many experimental investigations, including radiation shielding and interactions of radiation with matter. It may be used for X-ray fluorescence analysis, which requires a test sample of material to be irradiated with photons of appropriate energy, so that trace elements or impurities may be detected by the emission of fluorescent radiation.

The equipment includes a stabilised 300 kV constant potential power supply, a 300 kV X-ray tube, and a low energy 150 kV X-ray tube fitted with a beryllium window. The control console has provision for connection of laboratory quality meters to monitor operational parameters. X-ray beams of

sharply defined photon energy were obtained in the present work by two methods as follows:

(a) Filter Method in which the primary X-ray beam is modified by metal filters. Depending upon the arrangement of the apparatus either a standard "main beam" or a special "wide beam" may be produced.

(b) Radiator Foil Method in which thin metal foils are placed in the primary X-ray beam to obtain secondary beams of fluorescent radiation.

The two methods are described fully in Sections 2, 3 and 4 of this report, including filter and radiator foil design considerations, operational factors, and measured beam characteristics.

Particular care must be taken when using an X-ray generator for experimental radiation physics, to minimise the effects of both short and long-term fluctuations of the X-ray output, and to ensure that succe e test exposures are repeatable. The design and use of an X-ray transmis n monitor chamber and an electronic ratio device for this purpose are cribed in Section 5.

In some applications of the X-ray facility it is necessary know the exposure-rate at the test point in the radiation beam, for example in the calibration of civilian, military, or civil defence radiation measuring instruments. Methods for determining the true exposure-rate, and calibrating such instruments, were therefore considered, and these are described in Section 6.

A novel operating chart was devised for the "main beam" arrangement, which correlates the many operational factors in a convenient form. This chart is reproduced, in reduced size, in Fig. 2, together with explanatory notes. Development of the chart is described in the relevant sections of the report (ref. paras. 3.2, 3.5, 3.6, 3.8, 3.9 and 6.7).

Particular attention was given to radiation safety aspects of the facility. The control console and electronic instrumentation are located in a room adjacent to the exposure-room. The walls of these rooms are of substantial concrete and brick construction. A radiation survey was made with a Victoreen Model 440 Low Energy Survey Meter. This verified that any radiation dose received by personnel outside the exposure-room would be small, and well within internationally accepted dose limits, with the X-ray generator in normal operation. The sliding lead-shielded exposure-room door is fitted with a Castel interlock of the key X and key Y type. Key X is required to turn on the high voltage power supply at the console, and is only available for this purpose if the door is closed and locked. Key Y enables a person to ensure, by carrying the key with him, that the door cannot be locked and the X-ray generator operated, while he is inside the exposure-room. As a further safeguard warning lights, a buzzer, and an emergency stop switch are mounted in the exposure-room, together with a suitable warning notice. A telephone extension is also provided inside the exposure room.

2. PRIMARY X-RAY BEAMS : FILTER DESIGN

2.1 Primary X-ray Emission

When high energy electrons are incident on the target of an X-ray tube (ref. Fig. 3) bremsstrahlung (braking radiation) is produced as a result of deceleration of the electrons in the electrostatic fields of target nuclei and electrons. This radiation has a continuous spectrum of photon energies up to a maximum E_o keV, numerically equal to the tube voltage V_o kV. According to Playle [1] the spectrum is given by the equation:

$$N(E) = KI(E_o - E) \qquad (1)$$

where $N(E)$ = number of photons of energy E keV,
I = tube current,
and K = tube constant.

Fluorescent radiation from the target material is also produced as a result of the removal of inner shell electrons of target atoms. This radiation appears as a peak superimposed on the continuous spectrum, and for a tungsten target has a characteristic photon energy of about 61 keV.

2.2 Filter Design Criteria

Fig. 4 shows the effect of the inherent filtration of the tube on the X-ray output, and how the energy spectrum may be sharpened by the addition of a suitable external filter. In determining the optimum conditions, workers employing this method have used either the intensity or the effective energy of the photon beam as a criterion, the effective energy E_f keV being defined by standard half-value-layer (HVL) measurements. Playle, for example, selected a set of filters and corresponding tube voltages so as to obtain suitable effective energies. He obtained a useful range of exposure-rates by varying the tube current and/or test distance. According to Jones and Benyon [2] about 80% of the exposure-rate in such beams is due to photons within a "resolution band" $\pm$ 100 W/E_f % about the median energy, where W keV is the full width of the photon energy spectrum at half the maximum intensity. They state that E_f varies linearly with V_o, and that the usefulness of a given filter is limited to a total range of about 80 kV. Outside this range the energy spectrum becomes too broad at the higher voltages, and the intensity too low at the lower voltages.

2.3 Modal Energy

Jones and Benyon indicate that the effective energy of heavily filtered X-ray beams corresponds closely to the median energy. In the present work the modal energy is used to describe the energy of the beam. The modal energy is easily determined from spectrum measurements, being the point of maximum intensity. Since the spectra concerned are almost symmetrical, the three energy parameters "effective energy", "median energy", and "modal energy" are approximately equal.

2.4 X-ray Spectral Purity

Jones and Benyon have pointed out that to obtain acceptable spectral purity in the beam, care must be taken to reduce leakage radiation from the X-ray tube, especially as the beam intensity itself is substantially reduced by the heavy filter. In the present work it was found necessary to supplement the internal lead lining of the tube (ref. Fig. 3) with a layer of lead sheet 9.5 mm thick, wrapped around the central portion of the tube. Care must also be taken to reduce scattered radiation in the beam by collimating it so that it will be clear of side walls, floor, and surrounding objects. The collimators also reduce the amount of scattered radiation from the end wall of the exposure-room; for example, Jager [3] obtained a three-fold reduction in back-scattered radiation by this means. According to Aitken and Dixon [4] the use of collimators does not introduce a significant amount of unwanted radiation into the filtered beam.

2.5 Main and Wide Beams

Two holders were designed for attachment to the X-ray tube. The "main beam" holder provides mountings for the filter, two lead collimators, and the transmission monitor chamber, as shown in Fig. 5. In this arrangement the port on the side of the holder may be closed by a lead cover. The two collimators provide a well-defined conical X-ray beam, which is clear of scattering materials over the full range of test distances. The same holder is used for the fluorescent beams as shown in Fig. 6 (ref. para. 4.3). The second holder (not shown) is a smaller one with provision for a single lead collimator which is mounted close to the X-ray tube window. This wide aperture collimator provides a "wide beam" arrangement, which allows the irradiation of relatively large objects close to the X-ray tube. The transmission monitor chamber may also be used with the "wide beam" holder. The "wide beam" is not useful for test distances greater than about 2 m, owing to scattered radiation from surrounding materials.

2.6 Composite Filters

It is not possible to use a single filter material over the entire range of operating conditions required. Materials of higher atomic number Z must be used as the tube voltage is increased, and the penetrating power of the X-rays increases. Materials commonly used are aluminium (Z = 13), copper (Z = 29), tin (Z = 50), and lead (Z = 82). These are cheap, readily available, do not deteriorate rapidly by oxidation, and are easily machined. In the present work the attenuation factor T of a filter for photons of energy E was related to its thickness x cm by the equation:

$$T = e^{-\mu(E)x} = e^{-\frac{\mu}{\rho}(E)\rho x} \qquad (2)$$

where $\mu(E)$ = narrow beam linear attenuation coefficient, cm^{-1}

$\frac{\mu}{\rho}(E)$ = narrow beam mass attenuation coefficient, cm^2/g

and ρ = density of the material, g/cm^3

Values of $\mu/\rho(E)$ were obtained from the compilations of Hubbell [5] and Veigele et al [6]. To avoid unwanted peaks in the energy spectrum of the filtered beam due to fluorescent radiation produced in the filter material, it is necessary to use composite filters with components of successively lower Z material. The K X-rays of lead (energy about 77 keV) are largely absorbed by 3 mm of tin; those of tin (about 26 keV) by 0.5 mm of copper, and those of copper (about 8 keV) by 0.5 mm of aluminium, in each case the reduction factor being about 1000. The K X-rays of aluminium (energy about 1.5 keV) are absorbed in a few centimetres of air.

2.7 Transmission Peaks

As shown in Fig. 7 there is a discontinuity in the attenuation coefficient of a material at the K_{ab} photon energy, due to the onset of K-shell photoelectric interactions. For lead and tin the K_{ab} energies are about 88 and 29 keV, respectively. If the incident X-ray beam has an appreciable number of photons in this energy region, the transmitted beam will have an unwanted peak with a continuous spectrum of energies just below the K_{ab} energy. Lavender et al [7], after Jones [8], have shown that the tube voltage should be more than twice the K_{ab} energy of the first filter component to avoid such "transmission peaks".

2.8 Standard Filter Set

Taking into account the considerations above, a comprehensive set of thirty composite filters was designed, and these were designated systematically by a code number ea (ref. Table 1). The first letter e is an "energy index" which indicates, as a multiple of 50 kV, the high voltage design centre V_c kV of the filter. The useful range of the filter is approximately $V_c \pm 40$ kV. The second letter a is an attenuation index which indicates, as a power of ten, the attenuation factor of the filter for photons of energy numerically equal to $V_c/2$. Thus, for example, filter number 23 is designed for a high voltage of 100 ± 40 kV, and has an attenuation factor of 1000 for 50 keV photons. The greater the value of the attenuation index a, the sharper is the energy spectrum of the transmitted X-ray beam, but the intensity is also reduced. The set of filters with a = 3 appears to offer the best compromise between sharpness of peak and beam intensity, and this was selected as a standard set. In each of the thirty composite filters, the fluorescent radiation of each component is reduced by a factor of at least 1000 by the later components (ref. para. 2.6). The full set of 30 filters can be assembled from the 23 metal discs listed in Table 2.

2.9 Measured Spectra

X-ray spectra measured in the "main beam" are shown in Figs. 8(a) to (o). These were obtained with a collimated 3 inch long by 3 inch diameter NaI(Tl) scintillation spectrometer and 400 channel pulse height analyser (ref. Fig. 9). The energy scale of the analyser was calibrated against standard spectra from radioactive sources (ref. Figs. 8(p) and (q)). Figs. 8(a) to (q) are pulse height spectra, and do not precisely indicate the X-ray photon energy spectra because of the limited energy resolution of the scintillation spectrometer. The effect is clearly shown in Figs. 8(p) and (q), in which the line spectra of the radioactive sources are transformed into gaussian

pulse height peaks. Despite this smearing effect the modal energies of the X-ray beams can be determined with acceptable accuracy. For example, with filter number 43, a tube voltage of 200 kV, and a tube current of 50 μA, the modal energy is about 170 keV (ref. Fig. 8(h)). The small peak at about 77 keV in some of the spectra (see, for example, Fig. 8(i)) is due to fluorescent radiation from the lead collimator around the detector, and does not indicate a lack of spectral purity in the main beam.

3. PRIMARY X-RAY BEAMS : OPERATIONAL FACTORS

3.1 Air Attenuation and Air Density Correction Factors

The air attenuation correction factor A is used to allow for attenuation of the radiation between the X-ray tube and the test point. It depends upon the ambient temperature and pressure, and on the energy of the X-ray beam, and is most significant at the lower energies. To facilitate its determination the nomograph in Fig. 10 was constructed. This nomograph also provides the air density correction factor D, which is used to normalise the response of unsealed ionisation chambers to reference temperature and pressure conditions of 22°C and 101.3 kPa (1013 mbar) (ref. paras. 6.4 & 6.6).

3.2 Exposure-rate Constant

The exposure-rate $\dot{X}$ R/h at a point on the X-ray beam axis is proportional to the tube current I mA, and inversely proportional to the square of the test distance d m. Introducing a constant of proportionality Λ m^2.(R/h)/mA and including the air attenuation correction factor A, gives the equation:

$$\dot{X} = \frac{\Lambda I A}{d^2} \qquad (3)$$

The value of Λ depends upon the particular filter used and on the tube voltage. It was determined for the "main beam" for each of the filters 23 to 63, using the "standard instrument method" described in para 6.3. This was done for the range of modal energies covered by each filter, using a tube current of 1 mA. The experimental results, giving Λ as a function of the modal energy E for each filter, are given in the upper left-hand corner of the operating chart (ref. Fig. 2).

3.3 Scattered Radiation

The X-ray generator is set up in the exposure-room with the axis of the "main beam" 92 cm from a solid concrete and brick side wall. To check the effectiveness of the beam collimation system, the exposure-rate was measured at several distances from 1 to 6 m, using the standard instrument method (ref. para. 6.3). The monitor chamber was used to normalise the measurements against fluctuations in X-ray output (ref. paras. 5.1 and 5.2). The quantity $d^2\dot{X}/A$ was found to be independent of d up to 5 m, verifying the absence of significant scattered radiation. An increase in $d^2\dot{X}/A$ with d at greater distances was attributed to back-scattered radiation from the end wall, which is 6.6 m from the X-ray tube target.

3.4 Test Distance

Paragraph 3.3 indicates that the test distance should not exceed 5 m. The minimum test distance is governed by beam width considerations and the need for positional accuracy, especially as the beam intensity depends upon the square of the distance. Thus the minimum test distance is taken as 0.5 m.

3.5 Tube Current

The minimum tube current available with the 300 kV X-ray tube is about 50 μA at all tube voltages, while the maximum current depends upon the tube voltage as shown by the "Operating Region" curve given in the lower right-hand corner of the operating chart (ref. Fig. 2). The current is limited by the space-charge effects described by Jager [3] at voltages less than 200 kV, and by the 3 kW dissipation-rating of the X-ray tube at higher voltages. The maximum tube current is over 10 mA for all tube voltages above 50 kV. Adjustment of the tube current over its wide operating range is made by a filament current control on the console. A small change in the filament current causes approximately the same fractional change in the tube current at all operating points. Thus any value of tube current may be set with good precision. To obtain accurate readings of the tube current over the entire operating range, especially at the lower currents, the 0-15 mA panel meter on the console was supplemented in the present work by an external multi-range digital current meter.

3.6 Beam Intensity

For a selected filter and high voltage setting, the tube current and test distance can be varied independently over their respective ranges. The exposure-rate at the test point can therefore be varied through more than four orders of magnitude for most filters (ref. equation (3)). Moreover, since both the tube current and the test distance can be accurately measured, this wide range of exposure-rates is accurately reproducible. To facilitate selection of a mutually consistent set of parameters (Λ, I, d, $\dot{X}$) when using the "main beam", the nomograph on the left-hand side of the operating chart (ref. Fig. 2) was constructed. This links the four parameters through an intermediate parameter J, mA/m^2, which is given by the equation:

$$J = \frac{\dot{X}}{\Lambda} = \frac{I}{d^2} \qquad (4)$$

3.7 High Voltage and Tube Current

The output of the high voltage generator drops by about 2.7 kV per mA of tube current. A linear compensation circuit causes the reading of the high voltage meter to decrease at this rate when the tube current is increased. In the present work the high voltage control was adjusted to allow for this variation each time the current was altered. Nevertheless the spectrum measurements indicated that the modal energy of the "main beam" still varied with the tube current. This residual effect was investigated for filters 23, 33, 43, 53, and 63 using tube voltages of 100, 150, 200, 250, and 300 kV, respectively. In each case the tube current was varied over the full range available; the results are shown in Fig. 11. The "Set kV" and "Reference kV" are described in para. 3.8 below.

3.8 Set kV and Reference kV

The "set kV" S is the reading on the high voltage meter during the test exposure, at the actual tube current used, I mA. The "reference kV" K is the value of S that would give the same modal energy E, at a "reference current" of 50 μA. Fig. 11 shows that K (and therefore E) decreases for each filter with increasing tube current, even when S is kept constant. The experimental points were fitted by least squares for each filter to the equation:

$$K = b_0(S) + b_1(S) \log_{10} (I) \qquad (5)$$

The values of $b_0(S)$ and $b_1(S)$ so obtained were found to vary linearly with S, and using the method of least squares again, the following pair of equations was obtained (for I in μA):

$$\left.\begin{aligned} b_0(S) &= 1.108\ S - 3.45 \\ b_1(S) &= -0.0642\ S + 3.31 \end{aligned}\right\} \qquad (6)$$

This led to an overall result relating K to S and I given by the equation (for I in μA):

$$K = (1.108\ S - 3.45) - (0.0642\ S - 3.31) \log_{10} (I) \qquad (7)$$

The inclined "set kV" scale on the graph in the upper right-hand corner of the operating chart (ref. Fig. 2) was constructed to agree with this equation. This result clearly depends on the setting of the linear compensation circuit in the console (2.7 kV/mA), which should therefore be checked regularly.

3.9 Modal Energy and Reference kV

Spectrum measurements gave the modal energy E of the X-ray beam as the "reference kV" K was varied over the operating range (Vc ± 40 kV) of each filter. In each case, E was found to be a linear function of K. Linear regression gave the following equations:

$$\left.\begin{aligned} E &= 0.627\ K + 22.3, \quad \text{Filter 23} \\ &= 0.617\ K + 36.7, \quad \text{Filter 33} \\ &= 0.590\ K + 50.6, \quad \text{Filter 43} \\ &= 0.617\ K + 59.4, \quad \text{Filter 53} \\ &= 0.635\ K + 65.0, \quad \text{Filter 63} \end{aligned}\right\} \qquad (8)$$

Checks were made by measuring the modal energy at "set kV" values not used in deriving the equations, and at various tube currents up to the maximum available, for all the filters tested. This verified the equations, within the accuracy of the spectrum measurements of modal energy (1 or 2 keV). The linear relationship between E and K found in this work agrees with the results of Jones and Benyon [2] for effective X-ray energies found by half-value-layer (HVL) measurements. The set of equations (8) was used to construct the filter lines given in the graph in the upper right-hand quarter of the operating chart (ref. Fig. 2).

3.10 Beam Profiles

The X-ray intensity varies across the beam diameter owing to obliquity effects, especially if a heavy filter is used, and falls off quite sharply when the beam angle defined by the collimators is reached. Intensity profiles were obtained using a small ionization chamber detector mounted on a motor-driven platform as shown in the frontispiece. The scanning speed was slow enough to prevent distortion by the measurement system's time constant, and scans were made across the beam in both directions. To minimise the effect of fluctuations in X-ray output the monitor chamber and electronic ratio device (described in Section 5) were used. A light projector was used to define the X-ray beam axis. A typical profile scan is shown in Fig. 12.

3.11 Profile Function and Useful Beam Diameter

Data from the profile scans were used to construct Fig. 13, which gives the fractional reduction in beam intensity F(r) as a function of the radial distance r mm from the beam axis, for various X-ray beams and test distances. By selecting two parameters a and b for each test distance d it was found that the experimental points could be fitted by a profile function of the form:

$$F(r) = \exp\left[a\left\{1 - \sqrt{1 + (r/d)^b}\right\}\right] \qquad (9)$$

The useful beam diameter Δ may be defined as 2r where r is such that F(r) = 0.95 (ref. Fig. 12). The parameter Δ determines the minimum test distance for irradiation of objects of a given size: for example, referring to Fig. 13, this distance must not be less than about 2 m to irradiate a 200 mm radius circle in the main beam. To fully irradiate a cylindrical object of length L mm and diameter D mm, with its axis either parallel or perpendicular to that of the X-ray beam, Δ must exceed the minimum value Δ_c mm given by the equations:

$$\left.\begin{aligned} \Delta_c &= D \quad , \text{ co-axial case} \\ \text{or} \quad \Delta_c &= \sqrt{L^2 + D^2} \quad , \text{ perpendicular case} \end{aligned}\right\} \qquad (10)$$

4. FLUORESCENT X-RAY BEAMS

4.1 Fluorescent X-ray Emission

The fluorescent radiation beams are obtained by irradiating metal foils in the intense primary beam close to the X-ray tube. In the process of photoelectric absorption, the fluorescent X-rays of the foil material are produced, the most important being the K_α and K_β X-rays. The photon energies depend upon the foil material, and are less than 100 keV. The higher energy, less intense K_β X-rays may be preferentially attenuated by using a post-filter

with a K_{ab} energy lying between the highest K_α energy and the lowest K_β energy of the fluorescent radiation, as shown in Fig. 14. In designing post-filters Storm et al [9] chose an attenuation factor of 50 for the K_β X-rays, which results in an attenuation factor of up to 6 for the K_α X-rays. In the present work an attenuation factor of 20 for the K_β X-rays has been adopted. This gives a more useful fluorescent X-ray beam, as the maximum K_α attenuation factor is only 2.5, this occurring for a lead foil, as shown to scale in Fig. 14.

4.2 X-ray Spectral Purity

In principle it appears that a sharply defined energy peak can be obtained by this method. However, in practice the spectral purity of the fluorescent beam can be reduced by leakage radiation from the X-ray tube, and by Compton scattered radiation from the radiator foil and its mounting. Since the fluorescent beams are of lower intensity than the filtered beams, the leakage radiation must be reduced further. For this purpose the 9.5 mm thickness of lead sheet added to the central portion of the X-ray tube housing (ref. para. 2.4) was increased to 16 mm. In addition the cylindrical end parts of the tube were covered by 6 mm thick lead sheet, and the high voltage cable socket sections by 3 mm thick lead sheet. Fluorescent X-rays from the tungsten target can be Compton scattered in the radiator foil and give an unwanted peak in the fluorescent beam. For a fluorescent beam taken off at right-angles to the primary beam, this peak will occur at an energy of about 56 keV. It may be reduced in magnitude by employing a pre-filter of erbium: this material has a K_{ab} energy just below the energy of the tungsten fluorescent X-rays, and operates on the same principle as the post-filters described in para. 4.1. Bremsstrahlung from the tungsten target can also be Compton scattered in the radiator foil and this is more difficult to control. Most workers in this field have generally chosen thin radiator foils to reduce the intensity of this unwanted radiation in comparison with that of the fluorescent beam. However, Vyborny et al [10] refer to the use of foils "thick enough to absorb most of the primary radiation". The problem of obtaining the optimum spectral purity is discussed further below, in the paragraphs dealing with radiator foil thickness, radiator mounting angle, and tube voltage.

4.3 Fluorescent Beams

The fluorescent beam arrangement uses the same holder as the main beam arrangement (ref. Fig. 6). The first lead collimator, near the X-ray tube window, is replaced by one with a smaller aperture to avoid irradiation of the radiator foil mount and production of unwanted Compton scattered radiation. The fluorescent X-ray beam emerges from the side-port of the holder after passing through a post-filter, two further lead collimators, and the transmission monitor chamber. The lead cover is placed over the main port in order to attenuate the primary beam. Provision is made for the radiator foil to be placed at an angle of 45° to the primary beam, in either a "reflection" or a "transmission" mode. Ebert et al [11] have claimed that better spectral purity is obtained with the reflection mode for low-Z radiator foils, and with the transmission mode for high-Z radiator foils. However, this was not confirmed in the present work, and the reflection mode, which provides a fluorescent beam of greater intensity, was adopted as the standard configuration.

4.4 Radiator Foil Angle

In the photon energy range of interest (about 5 to 100 keV) the differential Compton scattering cross-section has a minimum at about 90°, and workers in this field universally agree that the fluorescent beam should be taken at this angle to the primary beam. Storm et al have shown that the most uniform fluorescent beam intensity profile is then obtained with the radiator foil inclined at 45° to each beam, and they report that the useful beam width increases linearly with the test distance. According to Kathren et al [12] a beam uniformity of 2% should be attainable in a well constructed system where the radiator foil and thickness do not vary by more than about 1% and 2%, respectively.

4.5 Tube Voltage

There is considerable conflict in the literature as to the best tube voltage to use with a given radiator foil. Kathren et al suggest that the kilovoltage should be no more than twice the atomic number Z of the radiator, in order to minimise the scattering of primary radiation. Storm et al differentiate between photon energy, photon flux, and radiation exposure-rate as criteria for X-ray spectral purity, and maintain that 300 kV yields the best spectral purity when radiation exposure-rate is the criterion. Vyborny et al, using a 150 kV X-ray tube, concluded that the optimum tube voltage varied with the K_{ab} energy of the radiator material, decreasing from 3 K_{ab} for low-Z materials to 2 K_{ab} for high-Z ones. On this basis their X-ray tube was limited to radiator foils with Z less than about 75, that is, tungsten, which has a K_{ab} energy of about 70 keV.

4.6 Radiator Foils and Post-Filters

A set of twelve radiator foils and matching post-filters was designed in the present work. These are listed in Table 3 including materials, thicknesses, average fluorescent radiation energies $\bar{E}_{K\alpha\beta}$ and $\bar{E}_{K\alpha'}$ and the K_α attenuation factors of the post-filters. Data are also given in Table 3 for the ^{68}Er pre-filter that may be used to reduce scattered radiation resulting from the tungsten fluorescent radiation. According to Kathren et al the optimum fluorescent to scattered radiation ratio is obtained with a radiator foil material of given atomic number Z if the mass thickness t mg/cm^2 is given by the equation:

$$t = 3.6\, e^{0.069Z} \qquad (11)$$

This function is shown in Fig. 15, together with a curve of t versus Z given by Storm et al, and the actual radiator foil thicknesses used by Ebert et al. The radiator foil thicknesses used in the present work are given approximately by the equation:

$$t = 13.5\, e^{0.046Z} \qquad (12)$$

and this function is also shown in Fig. 15.

4.7 Measured Spectra

X-ray fluorescent beam spectra obtained using the equipment described in para. 2.9 are shown in Figs. 16(a) to (l). The energy scale of the analyser was calibrated against the standard radioactive source spectra shown in Figs. 16(m) to (o). Note that the intensity scales are logarithmic, instead of linear as for the earlier main beam spectra. As an example of the difference Fig. 16(j) (with a linear scale) is included for comparison with Fig. 16(g).

4.8 Discussion of Results

These results indicate that useful X-ray beams can be obtained, although complete evaluation is not possible because of the limited energy resolution of the scintillation spectrometer, which fails to resolve the K_α and K_β X-rays of the radiator foils, and does not reveal the effect of the post-filters. If the results for each radiator foil are normalised to the same tube current, they show that the intensity of the Compton scattered radiation component increases more rapidly than does that of the fluorescent radiation peak as the tube voltage increases. This Compton scattered component would limit the usefulness of the beams for radiation instrument energy response studies. The scattered radiation would mask the response of such instruments to the fluorescent radiation at the nominal test energy, especially as the response tends to fall off at the lower energies. It appears from the present results that the optimum tube voltage is about 2.3 times the K_{ab} energy of the radiator foil, which gives a beam of useful intensity without excessive scattered radiation. This conclusion indicates higher tube voltages than those recommended by Kathren et al (ref. para. 4.5) for high-Z radiator foils, and much less than those indicated by the same workers for low-Z ones. Measurements made with an unshielded detector, using the lead radiator foil and a tube voltage of 300 kV, indicated that about 25% of the unwanted radiation in the spectrum is due to leakage radiation from the X-ray tube, the other 75% being scattered radiation from the foil. For the tin radiator foil and the same tube voltage these percentages are each about 50%.

4.9 X-ray Tubes

The present work was limited to use of the 300 kV X-ray tube. Further work is required using the low energy 150 kV beryllium-window X-ray tube with the low-Z radiator foils. This should also improve performance with the intermediate-Z foils such as niobium (ref. Figs. 16 (k) and (l). The low inherent filtration of the beryllium-window tube provides a beam with a significant number of photons having energies just above the K_{ab} energy of the low-Z radiator foils, giving good production of fluorescent radiation. If the primary beam has few photons in this critical energy region, compared with the number at higher energies, the fluorescent radiation will be small compared with the Compton scattered radiation. Ideally, to obtain the best signal to noise ratio for the wide range of radiator foils given in Table 3, it appears that two X-ray tubes are required with voltages of about 200 and 75 kV. Also, to obtain fluorescent beams of good intensity, high output X-ray tubes are required: for example, the 150 kV X-ray tube used by Vyborny et al [10] was rated at 50 kW.

5. X-RAY INTENSITY FLUCTUATIONS

5.1 X-ray Output Fluctuations

Line voltage variations, even after regulation, can cause significant fluctuations in the intensity of X-ray beams. Playle [1] found that heavily filtered beams were twice as sensitive to such variations as lightly filtered beams. It is necessary to ensure good regulation of both the primary voltage of the high voltage transformer, and the filament current. In the equipment described here the three phase mains supply is stabilised by a phase-shift transformer stabiliser, and then by a motor-driven auto-transformer controlled by an electronic stabiliser in the console. Fluctuations in X-ray output also occur because of the statistical nature of the X-ray production processes described in para. 2.1.

5.2 Monitor Chamber and Electronic Ratio Device

When using the X-ray facility it is necessary to ensure that test exposures are repeatable, and to minimise the effects of short and long-term fluctuations in X-ray output. Two devices provided for this purpose are:

(a) Transmission Monitor Chamber. This is an ionization chamber which may be mounted as shown in Figs. 5 and 6 so as to monitor either the primary or fluorescent X-ray beam. It enables test exposures to be normalised to any given reference exposure.

(b) Ratio Device. This device is used in connection with the testing of radiation measuring instruments. In conjunction with the monitor chamber it enables certain fluctuations in the response of the instrument to be eliminated, and the response to be normalised automatically to reference exposure conditions.

5.3 Monitor Chamber Design

Two transmission ionisation chambers were constructed, with vacuum deposited electrodes on the inner surfaces of the perspex walls. One was made with aluminium electrodes, and one with carbon. The saturation characteristics of the two chambers are similar, each requiring a minimum polarizing voltage of about 200 V. A small electrode spacing of about 6.4 mm was used without guard-rings, and there is an appreciable leakage current of 10 to 40 pA. This leakage current was found to vary only slowly with time, and a picoampere source may be used to approximately balance it out, enabling short-term measurements to be made with acceptable accuracy down to about 30 pA ionisation current. This limit of sensitivity corresponds to an exposure-rate of about 7.5 μC/kgh (30 mR/h) at a test distance of 5 m using the main beam. Thus the monitor chamber described cannot be used at the lower levels of X-ray output which are available (down to about 7.5 nC/kgh at 5 m test distance). Use of guard-rings to reduce the leakage current would improve the performance of such a chamber. A greater electrode spacing would also reduce this leakage current and, in addition, would provide greater sensitivity. However, increase of the electrode spacing is limited by the fact that each doubling of this spacing would require the polarizing voltage to be increased by a factor of four, if the collection efficiency is not to be reduced.

5.4 Ratio Device Operation

The electronic ratio device is based on a design published by Planskoy [13] which takes three input voltages X, Y, and Z and produces an output voltage W given by the equation:

$$W = XY/Z \tag{13}$$

In the present application X is derived from the instrument under test, either from an output socket or terminals, or from the terminals of a panel meter. Z is derived from the monitor chamber output. Y provides a scaling factor which enables measurements to be normalised to a previous reference exposure. Thus, in the test exposure, Y may be set to equal $\bar{Z}$, the mean value of the Z voltage obtained in the reference exposure. If, during the test exposure, both X and Z differ instantaneously from their mean values $\bar{X}$ and $\bar{Z}$ by independent factors a and b, and by common factor c, equation (13) gives:

$$W = XY/Z = ac\bar{X}Y/(bc\bar{Z}) = a\bar{X}Y/(b\bar{Z}) = a\bar{X}/b \tag{14}$$

Thus the output of the ratio device gives the mean response $\bar{X}$ of the instrument under test, normalised to the reference exposure $\bar{Z}$. Fluctuations which affect the instrument and monitor chamber equally (factor c) are completely cancelled, as shown by the typical recorder traces included in Fig. 17. Fluctuations (such as electrical noise) which occur independently in the instrument and the monitor chamber (factors a and b) are not cancelled out, and the W trace shows some small variations as a consequence. To facilitate the accurate determination of the mean level in the presence of these variations, a chart recorder is normally used to record the W output signal.

5.5 Measurement System Details

A block diagram of a complete measurement system employing the ratio device and monitor chamber is given in Fig. 17. Detailed circuit diagrams of the ratio device are given in Figs. 18 and 19. The cathode ray oscilloscope included in Fig. 17 is used for adjustment of the ratio device prior to measurements. This is done according to the procedure specified by the manufacturer of the integrated circuit used, employing a sine wave oscillator and a stable dc voltage source incorporated in the ratio device. The ionisation current from the monitor chamber is measured by a sensitive electrometer amplifier, the picoampere source being included to balance out the monitor chamber leakage current. The electrometer output is 30 V full scale; the gain of the Z input amplifier in the ratio device is therefore set at 1/3, so as to provide a standard 10 V full scale input. To provide the same standard input level, the gain of the X input amplifier is set at 10000/f, where f mV is the full scale output of the instrument under test. This instrument is connected to the ratio device through a buffer amplifier.

6. EXPOSURE-RATE DETERMINATION AND CALIBRATION OF RADIATION MEASURING INSTRUMENTS

6.1 Terms of Reference

Not all applications of the X-ray facility require knowledge of the exposure-rate at the test point; for example in shielding investigations, only the ratio of the X-ray intensities before and after the shield is required in order to determine a transmission factor. On the other hand, if the facility is to be used to test and calibrate radiation measuring instruments, the exposure rate at the test point must be known accurately. Three methods for determining the true exposure-rate and calibrating radiation measuring instruments will now be considered, including a number of correction factors. The methods are equally applicable to civilian, military and civil defence kinds of radiation protection instruments, and may easily be adapted to suit either radiation-rate or integrating types.

6.2 Operating Chart Method

When using the main beam, an estimate of the exposure-rate at the test point may readily be obtained from the operating chart (ref. Fig. 2). The accuracy of this method is low, partly because of the small scales on the chart and graphical limitations, and partly because fluctuations and drifts in the X-ray output may result in a somewhat different exposure-rate from that given by the chart. However, the method is useful for establishing operating conditions, and may be used for preliminary work.

6.3 Standard Instrument Method

The most accurate method of determining the exposure-rate at a test point in any of the available X-ray beams is to measure it directly with a calibrated instrument. In the present work a Farmer Secondary Standard Dosemeter with 0.6 and 30 cm^3 ionisation chamber detectors was used for this purpose. This instrument has a calibration traceable to the National Physical Laboratory (NPL) in the United Kingdom, and its accuracy was verified using a reference radioactive source of ^{90}Sr supplied with the instrument. It is noted that traceability to Australian primary standards could be effected by calibration of the instrument by the Australian Radiation Laboratory (ARL). Calibration of a radiation measuring instrument using the standard instrument method of true exposure-rate determination requires two consecutive exposures to be made, with the standard and test instruments placed in turn at the test point. To obtain the best accuracy the monitor chamber should be used to normalise the two exposures against any fluctuations or drifts in the X-ray output.

6.4 Correction Factors for the Standard Instrument Method

The air attenuation correction factor A (ref. para. 3.1 and Fig. 10) is not required when using the standard instrument method, as the exposure-rate is directly measured at the test point. The air density correction factor D (ref. para. 3.1 and Fig. 10) is required, if either the standard or the test instrument (but not both) employs an unsealed ionization chamber detector. If both instruments employ this type of detector, the correction factor D is not required.

If there is any significant difference between the dimensions of the detectors in the standard and test instruments, allowance should be made for X-ray beam non-uniformity. Frequently the detectors will be of cylindrical form, of length L mm and diameter D mm, exposed either co-axially or perpendicularly as shown in Fig. 20, and beam profile correction factors B(L,D) for these important cases will now be derived. If the detector is a low-pressure gas-filled ionization chamber the beam profile function F(r) (ref. para. 3.11) should be averaged over the chamber walls, as most of the secondary electrons giving rise to ionization in such chambers originate in the walls (ref. Attix [14] and Kondo and Randolph [15]). However, there is little error if the averaging is taken over the chamber volume, and this simpler procedure will be followed here. Since the variation of F(r) over the length of the cylinder will be small, the correction factor for the co-axial case is given by the integral:

$$B(L,D) = \frac{8}{D^2} \int_0^{D/2} r\, F(r)\, dr \qquad (15)$$

For the perpendicular case a double summation is required, and for this purpose the cylinder was divided into elements as shown in Fig. 21. The volume v_{ij} of any element ij, and its distance s_{ij} from the beam axis, are given by the equations:

$$v_{ij} = \delta^2 \sqrt{D^2/4 - r_i^2} \qquad (16)$$

and

$$s_{ij} = \sqrt{r_i^2 + l_j^2} \qquad (17)$$

Taking advantage of the eight-fold symmetry, the required correction factor is given by the summation:

$$B(L,D) = \frac{32}{\pi D^2 L} \sum_{i=1}^{D/2\delta} \left\{ v_{ij} \sum_{j=1}^{L/2\delta} F(s_{ij}) \right\} \qquad (18)$$

Values of B(L,D) obtained by this method for the main and wide beams were used to construct the graphs in Fig. 22, in which the correction factor B is shown as a function of the "equivalent co-axial diameter" Φ mm. For the co-axial case $\Phi = D$, and $B(\Phi)$ is given by the thick lines. It was found empirically that by taking $\Phi = \sqrt{L^2 + D^2}/1.3$, the thick lines could also be used for the perpendicular case; for comparison purposes the actual correction factors for the perpendicular case are indicated by the thin lines.

To facilitate determination of the parameter Φ and the beam profile correction factor B, the two nomographs in Figs. 23 and 24 were constructed. These nomographs also give the smallest useful beam diameter Δ_c mm that will fully irradiate the cylinders (ref. para. 3.11).

6.5 Accuracy of the Standard Instrument Method

Uncertainties in the standard instrument method of calibrating a radiation measuring instrument are summarised in Table 4, the various components being assessed as follows:

(a) Standard Instrument Calibration If the Farmer Dosemeter were calibrated at ARL, the systematic and random uncertainties would be about 2% and 1% respectively, and these values are given in Table 4. The uncertainty would be greater than this (about 5%) using the original NPL calibration supplemented by checks against the reference ^{90}Sr source.

b) Distance In the standard instrument method the aim is to locate the effective centres of the standard and test instruments at the same test distance, and the actual value of this test distance is irrelevant. The maximum percentage uncertainty in this procedure occurs at the minimum test distance of 0.5 m, and is estimated as a random uncertainty of about 1%.

(c) Test Instrument Response The uncertainty in this factor will depend upon the particular instrument being calibrated. However, for typical civilian, military, and civil defence instruments of both the radiation-rate and integrating types it is likely to be about 2% (random), and this value is given in Table 4.

(d) Normalisation The normalisation factor is the ratio of the monitor chamber outputs for the standard and test exposures. The greatest uncertainty will occur when relatively sensitive instruments are being calibrated, and the monitor chamber output is at a relatively low level. The uncertainty in the normalisation factor may then be as high as 2%, even if a chart recorder is used to enable fluctuations in the monitor current to be averaged out over each exposure. A random uncertainty of this magnitude is therefore included in Table 4.

Combining the component uncertainties as shown in Table 4 indicates an overall uncertainty of about 5%.

6.6 Monitor Chamber Method

In this method, the transmission monitor chamber is used as a tertiary standard of radiation measurement, for which purpose it must be calibrated against a secondary standard instrument. For any set of operating conditions, the exposure-rate $\dot{X}_M$ on the beam axis at a test distance d m, may be found from the monitor current M pA, using the equation:

$$\dot{X}_M = \frac{ACDM}{d^2} \qquad (19)$$

The factor C m^2.(mR/h)/pA is the monitor chamber calibration factor, and A and D are the air attenuation and air density correction factors (ref. para. 3.1 and Fig. 10). The air attenuation correction factor A is always needed in this method. However, care is required with the air density correction factor D. It should be used only if the test instrument being calibrated does not itself require an air density correction (for example, if it employs a sealed ionisation chamber). If the test instrument employs an unsealed ionisation chamber, the corrections for the monitor chamber (which is unsealed) and the test instrument will be equal and will cancel out.

A factor G is now introduced to provide for periodic checks of the system. If $\dot{X}_T$ is the true exposure-rate as determined by the standard instrument, then G is given by the equation:

$$\dot{X}_T = G\,\dot{X}_M = ACDGM/d^2 \qquad (20)$$

Equation (20) gives the exposure-rate on the beam axis. Using the beam profile correction factor B, the effective exposure-rate $\dot{X}_E$ appropriate to the calibration of a radiation detector of finite size is given by the equation:

$$\dot{X}_E = B\,\dot{X}_T = ABCDGM/d^2 \qquad (21)$$

6.7 Monitor Chamber Calibration Factor

Comparison of equations (3) and (19), shows that the parameters Λ and C are related by the equation:

$$C = \frac{I}{DM}\Lambda \qquad (22)$$

In the present work, C was determined directly from measurements of the true exposure-rate $\dot{X}_T$ using the Farmer Dosemeter. Using $\dot{X}_T$ in place of $\dot{X}_M$ in equation (19), and adding the beam non-uniformity correction factor B for the standard instrument, C is given by the equation:

$$C = \frac{d^2\,\dot{X}_T}{ABDM} \qquad (23)$$

For the Farmer Dosemeter the beam non-uniformity correction was negligible, being less than 0.2% at 1 m in the main beam. This calibration was done for the main beam, over a range of modal energies, for the standard set of filters. The values of C obtained were plotted against the modal energy, and the points were fitted by a smooth curve as shown in Fig. 25. Values of C for use in equations (20) and (21) may be taken from this curve. The results were found to be independent of exposure-rate, which was varied by using a range of X-ray tube currents from 500 μA to 9 mA , using filter number 53 at a modal energy of 223 keV. Corresponding monitor chamber calibration factors were not determined for the wide and fluorescent beams. Fig. 25 indicates that the value of C is roughly 33 $m^2.(mR/h)/pA$. This value was used to construct the F, M and $\dot{X}$ scales in the lower left-hand corner of the operating chart (ref. Fig. 2), in order to show the approximate relationship between $\dot{X}$, M, and d. The parameter F m^2R/h is given by the equation:

$$F = \dot{X}\,d^2 \doteq CM \quad (A,B,D,G \approx 1) \qquad (24)$$

Although only very approximate, the nomograph can be used to estimate the magnitude of the monitor current which will be obtained in a proposed exposure, allowing a suitable electrometer range to be selected.

6.8 Accuracy of the Monitor Chamber Method

Uncertainties in the monitor chamber method of calibrating a radiation measuring instrument using equation (21) are summarised in Table 5, the various components being assessed as follows:

(a) Monitor Chamber Calibration Taking into account the uncertainties associated with the Farmer Dosemeter quoted in para. 6.5(a), and an additional systematic uncertainty of about 2% in fitting the calibration curve to the experimental points in Fig. 25, indicates systematic and random uncertainties of about 2.8% and 1%, respectively. These values are given in Table 5.

(b) Monitor Chamber Current The greatest uncertainty in this factor occurs when relatively sensitive instruments are being calibrated, and the monitor chamber current is relatively small. The uncertainty in the current measurement may then be about 1%, even if a chart recorder is used to average out fluctuations. If several exposures are made using the electronic ratio device, the Y voltage is normally set to equal the mean monitor chamber signal Z as described in para. 5.4, and this involves a further uncertainty of about 0.5%, associated with the setting of the precision ten turn potentiometer. A total random uncertainty of about 1.1% is therefore assigned to this factor.

(c) Monitor Chamber Calibration Correction Use of the factor G is an artifice, the product CG representing an updated calibration of the monitor chamber. As such CG will have the uncertainty quoted in item (a) above. Hence no separate uncertainty is attached to G, and it is excluded from Table 5.

(d) Measuring System Stability Over a period of time between calibration checks against the standard instrument there may be changes in the characteristics of the monitor chamber, the electronic ratio device, or their associated electronics. To allow for this factor a random uncertainty of 2% is included in Table 5.

(e) Distance Uncertainty in fixing the origin of the distance measuring scale at the X-ray tube target contributes a systematic uncertainty of about 2.5 mm in the test distance. There is also a random uncertainty of about 2.5 mm in the location of the effective centre of the test instrument's radiation detector. The maximum percentage uncertainties in d^2 occur at the minimum test distance of 0.5 m, and are then about 1% (systematic) and 1% (random).

(f) Air Attenuation Correction Allowing an uncertainty of about 3 keV in the effective X-ray energy (taken as the modal energy from the operating chart, ref. Fig. 2), the air attenuation correction factor determined from the nomograph in Fig. 10, has negligible uncertainty (say 0.1% random) for energies above about 50 keV. However, the uncertainty increases significantly below this energy, due to the change in slope of the μ/ρ versus E curve, and is taken as 2.5% (random) at 30 keV, which is the minimum proposed energy for the main beam. These uncertainties are given in Table 5.

(g) Beam Profile Correction Uncertainty in this factor is not likely to exceed 0.2% (random).

(h) Test Instrument Response Assessment of this factor is as given in para. 6.5(c), and an uncertainty of 2% (random) as included in Table 5.

Combining the component uncertainties as shown in Table 5 indicates an overall uncertainty of about 7%. As may be expected this uncertainty is greater than that associated with the standard instrument method.

7. CONCLUSIONS AND RECOMMENDATIONS

An X-ray test facility has been established to provide a radiation beam of energy between 5 keV and 250 keV, using either composite filters to modify the primary X-ray spectrum, or radiator foils to produce secondary fluorescent X-rays. Exposure-rates available range from 7.5 nC/kg h (30 μR/h) to over 75 mC/kg h (300 R/h).

A range of composite filters has been designed for use with the 300 kV X-ray tube. Several of these (filters 13 to 63) have been selected as a standard set to provide a range of sharply-defined beam energies from 30 to 250 keV. Results from the detailed evaluation of filters 23 to 63 have been incorporated in a novel operating chart which combines operational factors (filter number, tube voltage, tube current, and test distance) to predict filtered X-ray beam characteristics (beam modal energy and exposure-rate). Some further work with filter 13 is recommended in order to complete evaluation of the standard set of filters. Also, to provide a wider choice of X-ray beam characteristics, it may be useful to evaluate the filters having ten times and one-tenth the attenuation factor of the standard set, ie filters 14 to 64 and 12 to 62, respectively.

A range of radiator foils and post-filters has been designed. Limited evaluation of some of these foils, using a 300 kV X-ray tube and a scintillation spectrometer, indicates that useful X-ray beams can be obtained by this method. It is recommended that this work be continued with a low energy 150 kV beryllium window X-ray tube, to extend the energy range down to 5 keV. High output X-ray tubes would provide more intense fluorescent X-ray beams. A 200 kV tube and a 75 kV beryllium-window tube are recommended. An important factor is the radiator foil thickness, and some research to establish its effect on beam intensity and spectral purity would be useful.

Throughout the work the modal energy has been used as a measure of the X-ray beam energy. It could be worthwhile carrying out some half-value-layer (HVL) measurements to verify that this modal energy approximates the effective energy.

Application of the test facility to the testing and calibration of radiation measuring instruments, including civilian, military, and civil defence types, has been considered in detail, and methods of calibration have been described. These methods include the use of a transmission monitor chamber and electronic ratio device to automatically correct results for X-ray

tube output fluctuations, and to normalise measurements to a reference exposure. The best accuracy that can be achieved in the calibration of an instrument is about 5%, requiring the use of a secondary standard instrument calibrated at the Australian Radiation Laboratory (ARL). Finally it is noted that the present monitor chamber has some limitations, and it is recommended that this be replaced by one of improved design.

8. ACKNOWLEDGEMENTS

I wish to acknowledge the support and encouragement given freely by many people during the various stages of the work described in this report. In particular, thanks are due to Mr E.F. Heywood of the RMIT, and to Mr J.W. Allison of MRL for many helpful discussions, and to the latter for his assistance in revising the text. Thanks are due to the Design Office of MRL for preparing engineering drawings of the hardware suggested by the author's sketches, and to those involved in the manufacturing processes. I would also like to thank the MRL technical illustrator for the painstaking preparation of the many diagrams, graphs and charts.

9. REFERENCES and BIBLIOGRAPHY

REFERENCES

1. Playle, T.S. (1964). "A 250 kV X-ray set for Dosemeter Calibration". Report RD/B/N213. Central Electricity Generating Board, Berkeley Nuclear Laboratories.

2. Jones, E.W. & Benyon, D.E. (1971). "Spectral Distribution of Filtered X-Ray Radiation Generated at Constant Potentials from 100 kV to 300 kV". Report DREO TN 71-22. Defence Research Establishment Ottawa.

3. Jager, W.F. (1962). "A Standardised Source of 23-200 keV X-Radiation". Report ARL/R9/C. Admiralty Research Laboratory, Teddington.

4. Aitken, J.H. & Dixon, W.R. "X-Ray Spectra from a 100 kV Machine". Report APXNR-562. National Research Council of Canada.

5. Hubbell, J.H. (1969). "Photon Cross-Sections, Attenuation Coefficients, and Energy Absorption Coefficients from 10 keV to 100 GeV." Circular NBS-29. National Bureau of Standards.

6. Veigele, W.J., Briggs, E. & Bates, L. (1971). "X-Ray Cross-Section Compilation from 0.1 keV to 1 MeV Discussion, etc." Report AD 890 434L. Kaman Sciences Corp.

7. Lavender, A., Thompson, I.M.G., Shipton, R.G. & Goodwin, J. (1969). "Modification of the BNL 250 kV X-Ray Set and the Recalibration of its Output". Report RD/B/N 1263. Central Electricity Generating Board, Berkeley Nuclear Laboratories.

8. Jones, D.E.A. (1961). Brit. J. Radiol. 34, 801.

9. Storm, E., Lier, D.W. & Israel, H.I. (1974). "Photon sources for instrument calibration". Health Physics 26, 179-189.

10. Vyborny, C.J., Dol, K., Metz, C.E. & Haus, A.G. (1977). "A simple source of fluorescent X-rays for the study of radiographic imaging systems". Med. Phys. 4 (6), 482-485.

11. Ebert, P.J., Gaines, J.L. & Leipelt, G.R. (1972). "Production of Monoenergetic X-Ray Sources of Known Absolute Intensity". Nucl. Instrum. Methods 99, 29-34.

12. Kathren, R.L., Rising, F.L. & Larson, H.V. (1971). "K-Fluorescence X-Rays : A Multi-Use Tool for Health Physics". Health Physics 21, 285-293.

13. Planskoy, B. (1972). "Ratio Circuit for Plotting Dose Distributions in the Radiation Field of the 8 MV MEL Linear Accelerator". Brit. J. Radiol. 45, 543-546.

14. Attix, F.H. & Roesch, W.C. (eds.) (1966). Radiation dosimetry. Academic Press.

15. Kondo, S. & Randolph, M.L. (1960). "Effects of finite size of ionisation chambers on measurements of small photon sources". Rad. Res. 13, 37-60.

BIBLIOGRAPHY

Cember, H. (1969)
Introduction of health physics.
Pergamon Press.

Gaines, J.L., Ebert, P.J., Leipelt, G.R.
"Detector calibration techniques, X-ray machine intensities and fluorescent X-ray spectrum catalog." Report UCID-16091.
Lawrence Livermore Laboratory.

Lapp, R.E., Andrews, H.L. (1963)
Nuclear radiation physics.
Pitman.

Lederer, Hollander, Perlman. (1968).
Table of isotopes, 6th ed.
Wiley.

Lier, D.W., Israel, H.I., Storm, E. (1972).
"Measurements of filtered X-ray spectra". Report LA-4878.
Los Alamos Scientific Laboratory.

Shambon, A. (1974).
"Narrow energy band filters for a 250 kV constant potential X-ray machine". Report HASL-279.
United States Atomic Energy Commission Health and Safety Laboratory.

Storm, D., Lier, D.W. (1972).
"X-ray spectral distributions in roentgens".
Health Physics 23, 73-84.

Stretton, J.S. (1965)
Ionising Radiations.
Pergamon Press.

TABLE 1

COMPOSITE FILTERS

Each composite filter is assembled in the order shown, with the element in the first row being placed nearest to the X-ray tube

Filter Number[1] (e \ a)	Thickness (mm)					Material
	1	2	3[2]	4	5	
1	0.15 0.5	0.30 0.5	0.45 0.5	0.60 0.5	0.75 0.5	Copper Aluminium
2	1.0 0.5	2.0 0.5	3.0 0.5	4.0 0.5	5.0 0.5	Copper Aluminium
3	0.5 1.0 0.5 0.5	0.5 2.0 0.5 0.5	0.5 3.0 0.5 0.5	0.5 4.0 0.5 0.5	0.5 5.0 0.5 0.5	Aluminium[3] Tin Copper Aluminium
4	0.5 - 2.0 0.5 0.5	0.5 - 4.0 1.0 0.5	0.5 - 5.0 4.5 0.5	0.5 1.0 3.0 0.5 0.5	0.5 1.0 5.0 1.0 0.5	Aluminium[3] Lead Tin Copper Aluminium
5	0.5 - 3.0 2.0 0.5	0.5 - 5.0 7.0 0.5	0.5 1.0 5.0 2.5 0.5	0.5 2.0 4.0 0.5 0.5	0.5 2.5 5.0 1.0 0.5	Aluminium[3] Lead Tin Copper Aluminium
6	0.5 - 5.0 2.0 0.5	0.5 1.0 5.0 3.0 0.5	0.5 2.5 4.0 0.5 0.5	0.5 3.5 4.0 1.0 0.5	0.5 4.5 4.0 2.0 0.5	Aluminium[3] Lead Tin Copper Aluminium

Notes: (1) e = Energy Index; a = Attenuation Index (see text)

(2) Standard set (see text)

(3) 0.5 mm aluminium is used to protect the lead and tin discs from abrasion.

TABLE 2

COMPONENTS FOR COMPOSITE FILTERS IN TABLE 1

Thickness (mm)	Number of Discs			
	Aluminium	Copper	Tin	Lead
0.15	-	5	-	-
0.5	2	1	-	-
1.0	-	7	5	2
2.5	-	-	-	1

TABLE 3

RADIATOR FOILS, POST-FILTERS, AND ERBIUM PRE-FILTER

Radiator Foil				Post Filter[1]		
Element	Thickness (μm)	$\bar{E}_{K\alpha\beta}$[2] (keV)	$\bar{E}_{K\alpha}$[3] (keV)	Element	Thickness (μm)	Mean K_α Attenuation Factor
^{22}Ti [5]	80	4.55	4.51	-	-	-
^{25}Mn	60	5.95	5.90	^{24}Cr	2.7	1.14
^{29}Cu [5]	60	8.13	8.04	^{28}Ni	3.9	1.19
$Na^{35}Br$	270	12.09	11.91	^{34}Se	19	1.32
^{41}Nb [5]	100	16.90	16.59	^{40}Zr [5]	20	1.28
^{47}Ag [5]	110	22.58	22.10	^{45}Rh	26	1.43
^{50}Sn [5]	175	25.77	25.19	^{48}Cd [5]	50	1.49
^{58}Ce	290	35.5	34.6	^{57}La	120	1.67
^{62}Sm	320	41.0	39.9	^{60}Nd	140	1.72
^{69}Tm	350	51.9	50.4	^{66}Dy	170	1.75
^{78}Pt	240	68.4	66.2	^{74}W	130	1.89
^{82}Pb [5]	500	76.7	74.2	^{79}Au	180	2.56
^{74}W	X-ray tube target	60.7	Pre-filter	^{68}Er	200	3.45 [4]

Notes:

(1) Designed for a K_β attenuation factor of 20.

(2) $\bar{E}_{K\alpha\beta}$ = Mean energy of K_α and K_β X-rays.

(3) $\bar{E}_{K\alpha}$ = Mean energy of K_α X-rays.

(4) Mean attenuation factor of tungsten K_α and K_β X-rays.

(5) Only these foils obtained in present work.

TABLE 4

UNCERTAINTIES IN CALIBRATION OF A RADIATION MEASURING INSTRUMENT BY THE STANDARD INSTRUMENT METHOD

Component	Uncertainty in exposure-rate, %	
	Systematic	*Random*
Standard Instrument Calibration	2	1
Distance	-	1
Test Instrument Response	-	2
Normalisation	-	2
Sum in Quadrature	2	3.2
Total (Systematic + Random)	5.2	

TABLE 5

UNCERTAINTIES IN CALIBRATION OF A RADIATION MEASURING INSTRUMENT BY THE MONITOR CHAMBER METHOD

Component	Uncertainty in exposure-rate, %	
	Systematic	Random
Monitor Chamber Calibration	2.8	1
Monitor Chamber Current	-	1.1
Measuring System Stability	-	2
Distance	1	1
Air Attenuation Correction	-	2.5% at 30 keV 0.1% above 50 keV
Beam Profile Correction	-	0.2
Test Instrument Response	-	2
Sum in Quadrature	3.0	4.2 at 30 keV 3.4 above 50 keV
Total (Systematic + Random)		7.2 at 30 keV 6.4 above 50 keV

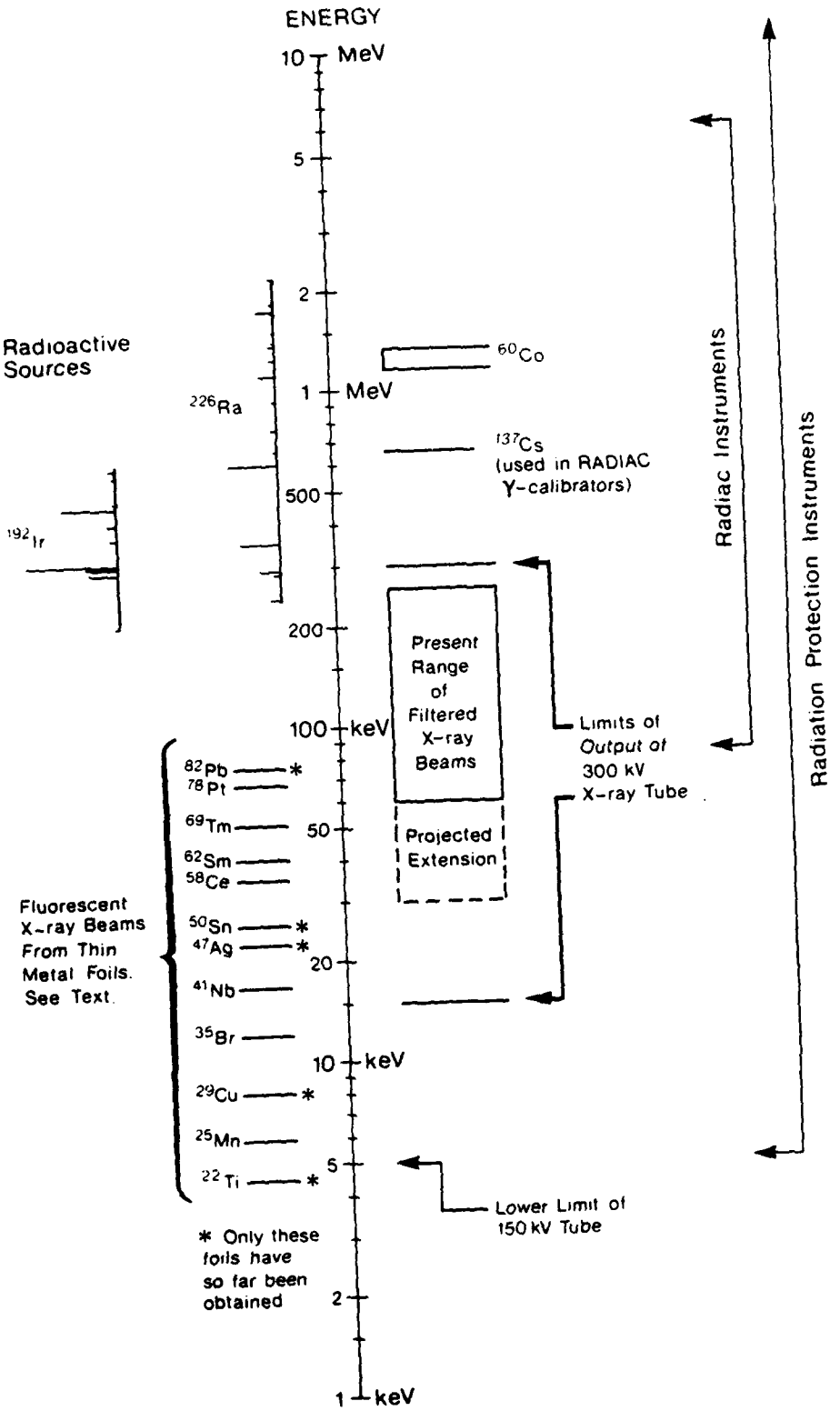

FIG. 1 - Photon energy ranges of test facilities and radiation measuring instruments.

The spectra of the radioactive sources ^{192}Ir, ^{137}Cs, ^{226}Ra, and ^{60}Co are shown to scale, 1 photon/disintegration = 20 mm.

FIG. 2 OPERATING CHART FOR THE MAIN BEAM ARRANGEMENT

Example and Explanatory Notes

Example:

Determination of suitable operating conditions for exposure of a 300 mm diameter radiation detector to a beam with a modal energy of 173 keV and an exposure-rate of 200 mR/h, and estimation of the monitor chamber current to enable a suitable instrument range to be selected.

Procedure:

(a) Step 1 on the chart indicates filter number 43 for E = 173 keV.

Note 1: Sometimes a choice of filter will be available (eg. if E = 180 keV): the higher-numbered filter will then provide the sharper energy peak but a lower beam intensity.

Note 2: Step 2 indicates that the maximum exposure-rate available is approximately 100 R/h.

(b) Step 3 indicates an exposure-rate constant Λ = 1.6 m^2.(R/h)/mA and step 4 combines this with $\dot{X}$ = 0.2 R/h to obtain J = 0.13 mA/m^2.

(c) In step 5 a suitable pair of values of tube current I and test distance d must be selected subject to the following constraints:

(i) I must not exceed the maximum rated current I_{MAX}. To check this steps 6 and 7 are followed to obtain reference kV K = 207, and the set kV S is approximated by the value S_1 = 1.1 K = 228. Using the Operating Region curve I_{MAX} is therefore approximately 14 mA. If required this estimate may be improved in accuracy following item (d) below.

(ii) Reference to Fig. 24 indicates that d must be greater than 1.5 m if the useful beam diameter Δ is not to be less than the 300 mm diameter of the test object.

(iii) In general, the maximum value of d should be chosen, as this gives the maximum monitor chamber current, and therefore the best measurement precision in both this quantity and the distance itself.

In the example shown on the chart I = 3.2 mA and d = 5.0 m are selected.

(d) Steps 8 and 9 use the last-mentioned values to obtain the actual set kV S = 225.

(e) Finally, step 10 uses the values d = 5.0 m and $\dot{X}$ = 0.2 R/h to obtain the estimated monitor chamber current M = 180 pA.

Conclusion:

The radiation detector should be located with its effective centre at a test distance of 5.0 m. The monitor chamber electrometer should be set to a range consistent with an expected current of about 180 pA. Filter number 43 should be used. During the exposure the tube current and high voltage controls should be adjusted so that the corresponding console meters read 3.2 mA and 225 kV, respectively.

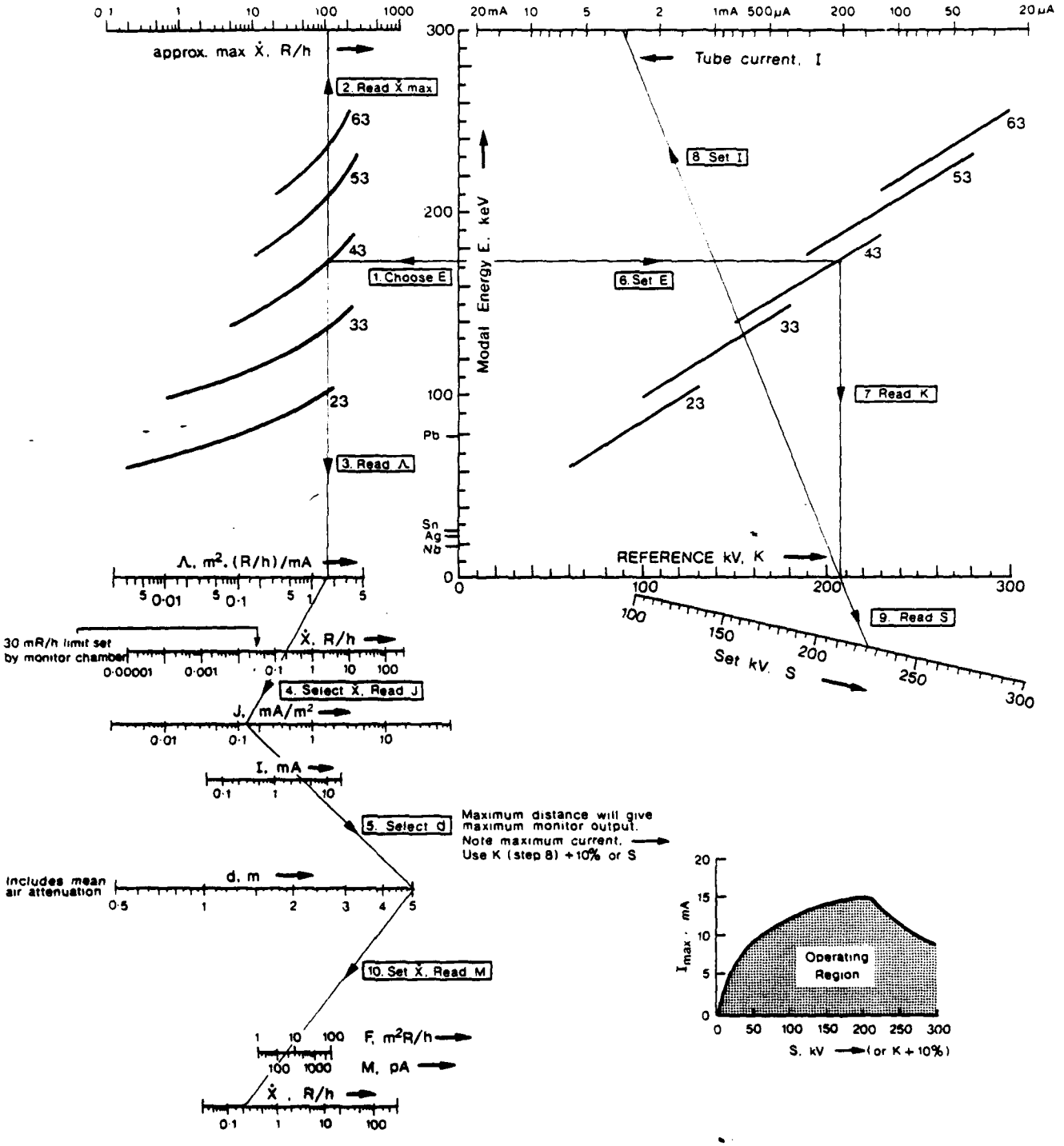

FIG. 2 - Operating Chart for the main beam arrangement (Reduced Size)

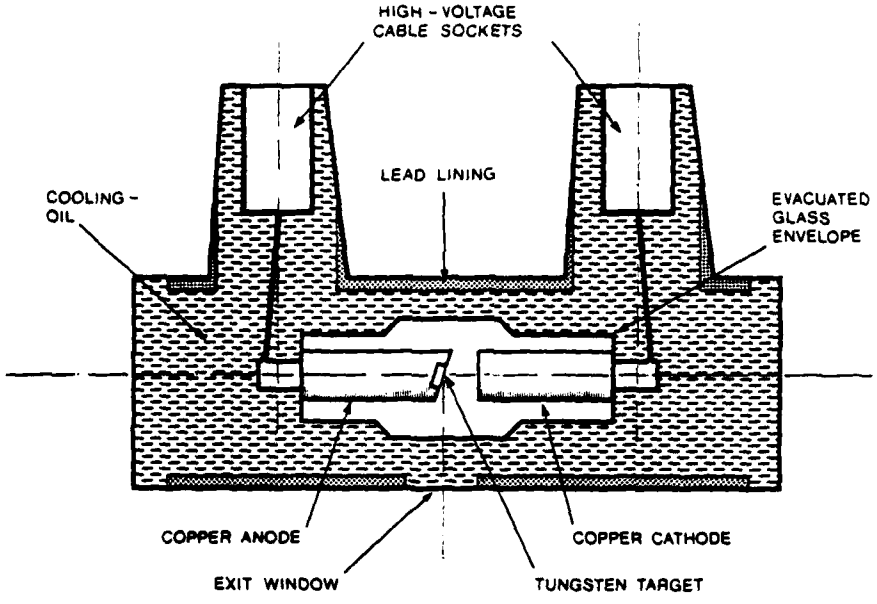

FIG. 3 - Schematic diagram of 300 kV X-ray tube.

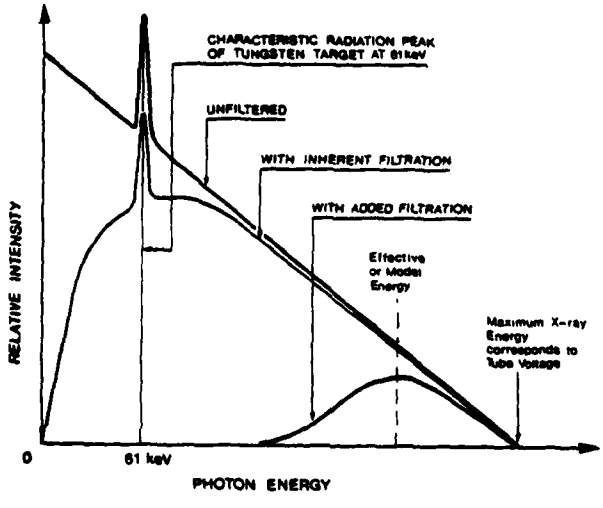

FIG. 4 - Effect of inherent and added filtration on X-ray tube emission spectrum.

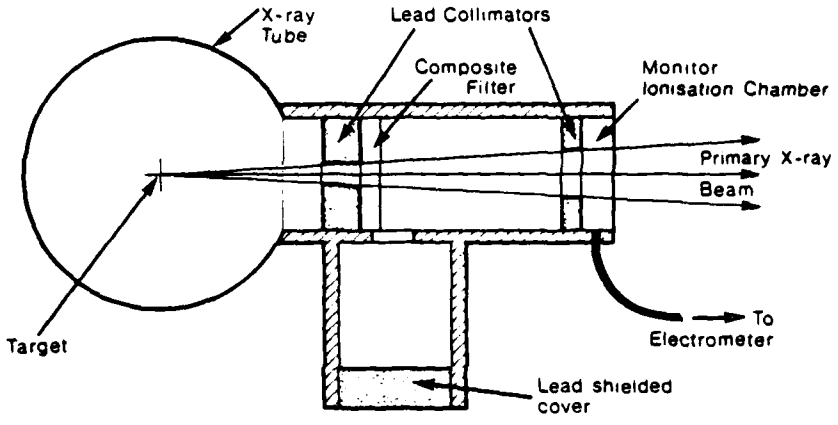

FIG. 5 - X-ray tube attachement as set-up for the main X-ray beams.

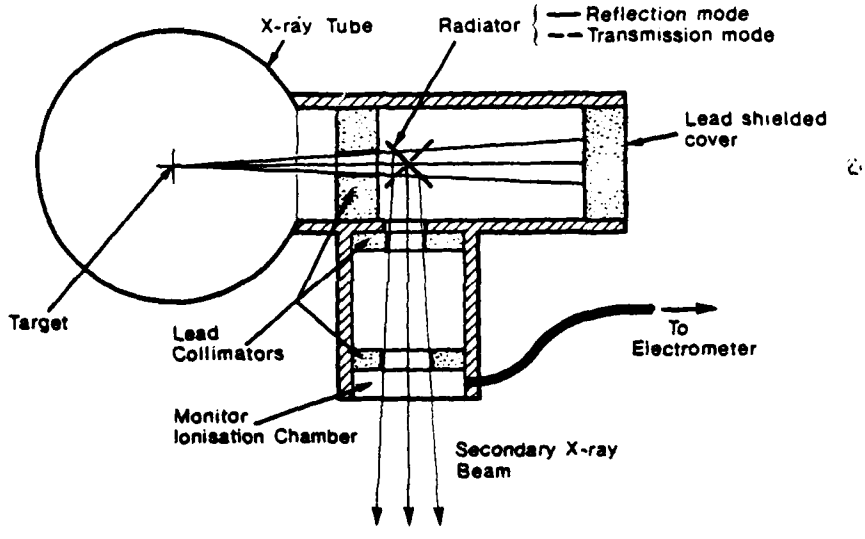

FIG. 6 - X-ray tube attachment as set-up for the fluorescent X-ray beams

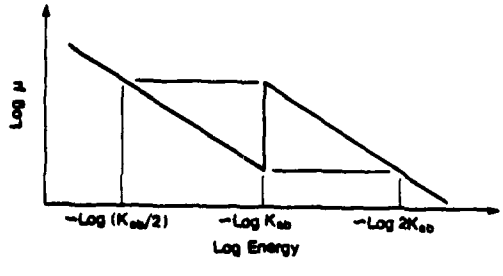

FIG. 7 - Variation of the linear attenuation coefficient μ at the K_{ab} photoelectric absorption edge.

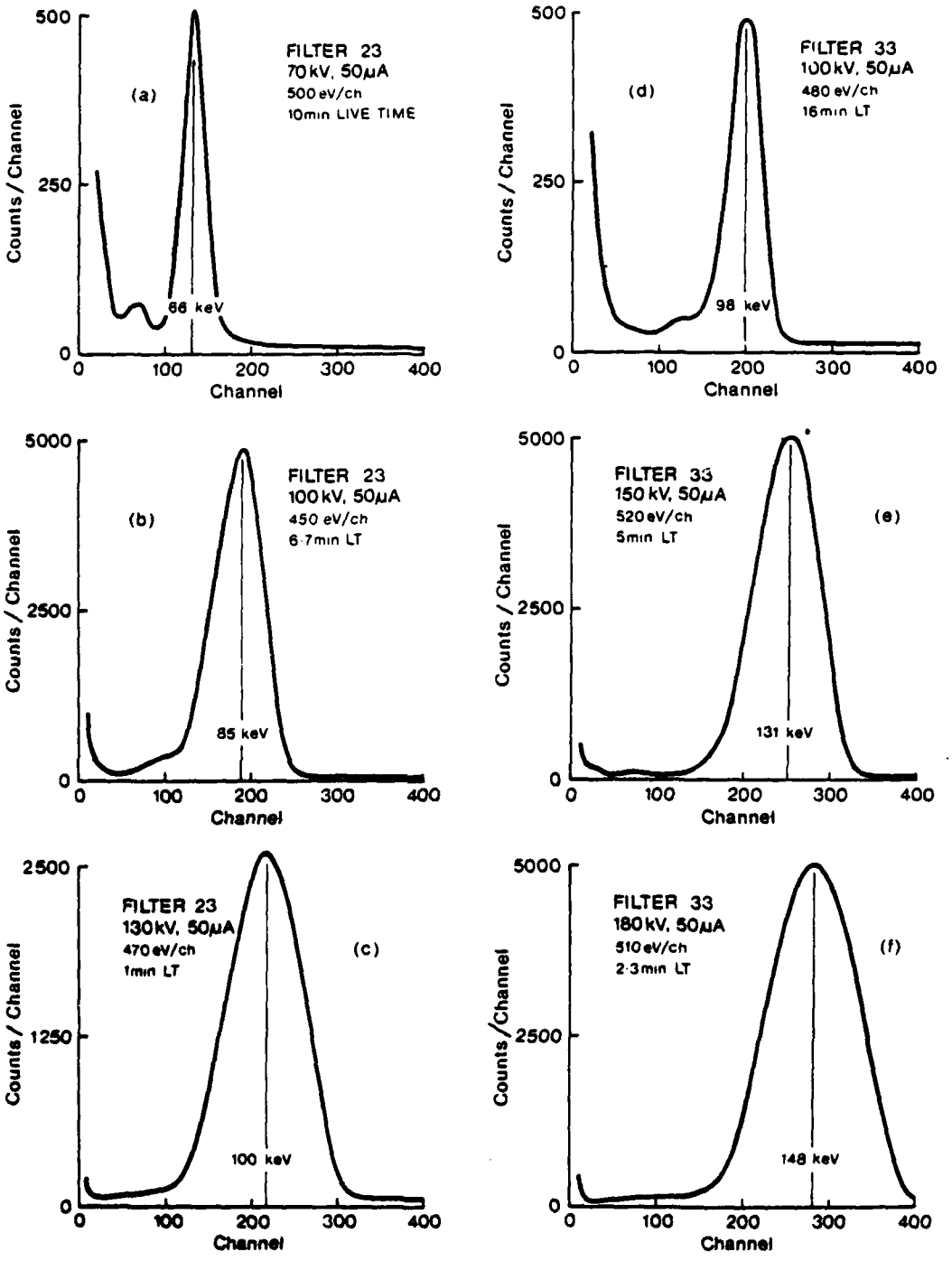

FIG. 8 - Typical main X-ray beam measured spectra and radioactive source calibration spectra

Part 1: X-ray beam examples (a) to (f)

Data includes filter number, set kV, tube current, and multi-channel analyser sensitivity (eV/ch) and live time (LT).

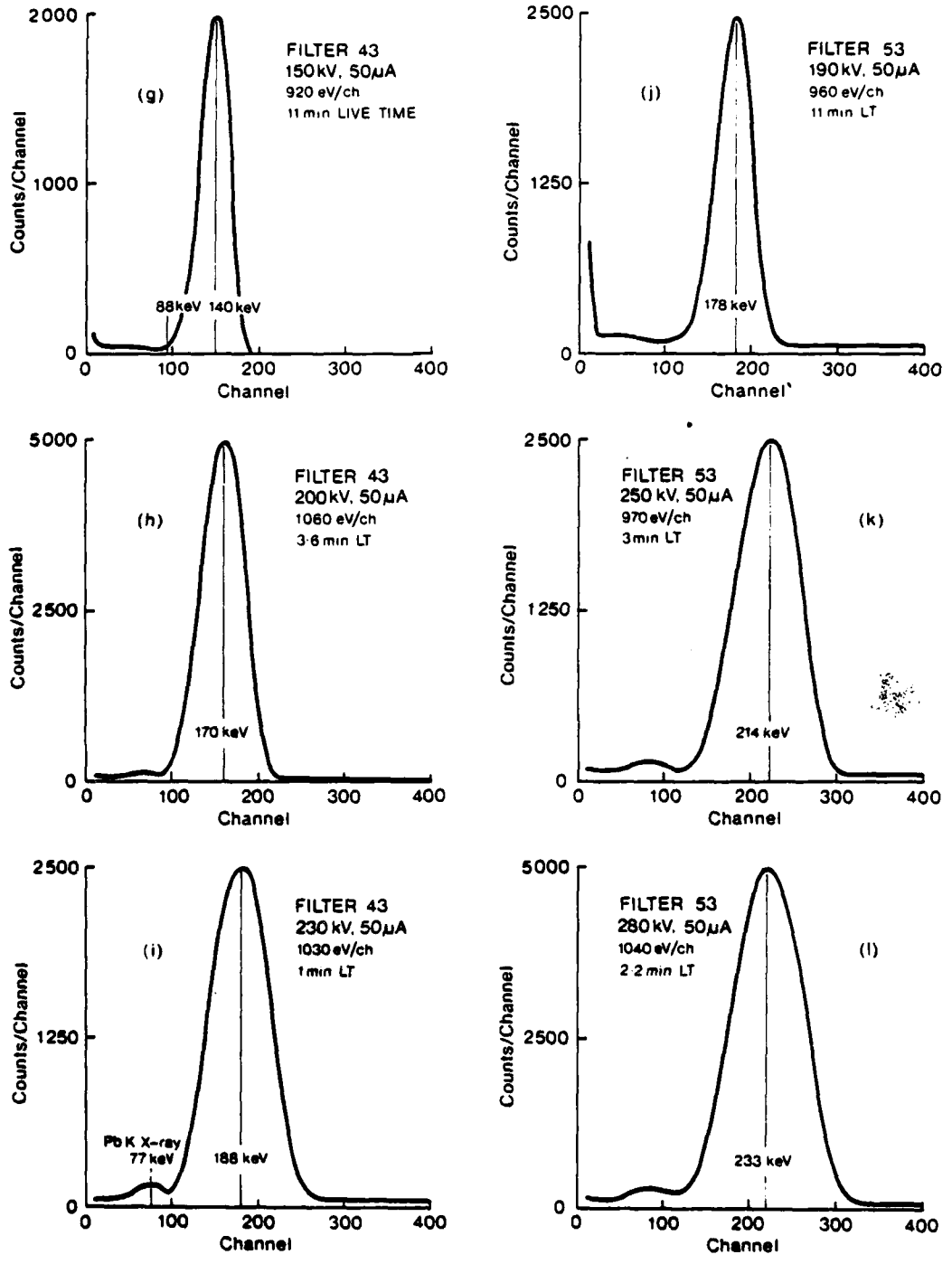

FIG. 8 - Typical main X-ray beam measured spectra and radioactive source calibration spectra

Part 2: X-ray beam examples (g) to (l)

Data includes filter number, set kV, tube current, and multi-channel analyser sensitivity (eV/ch) and live time (LT).

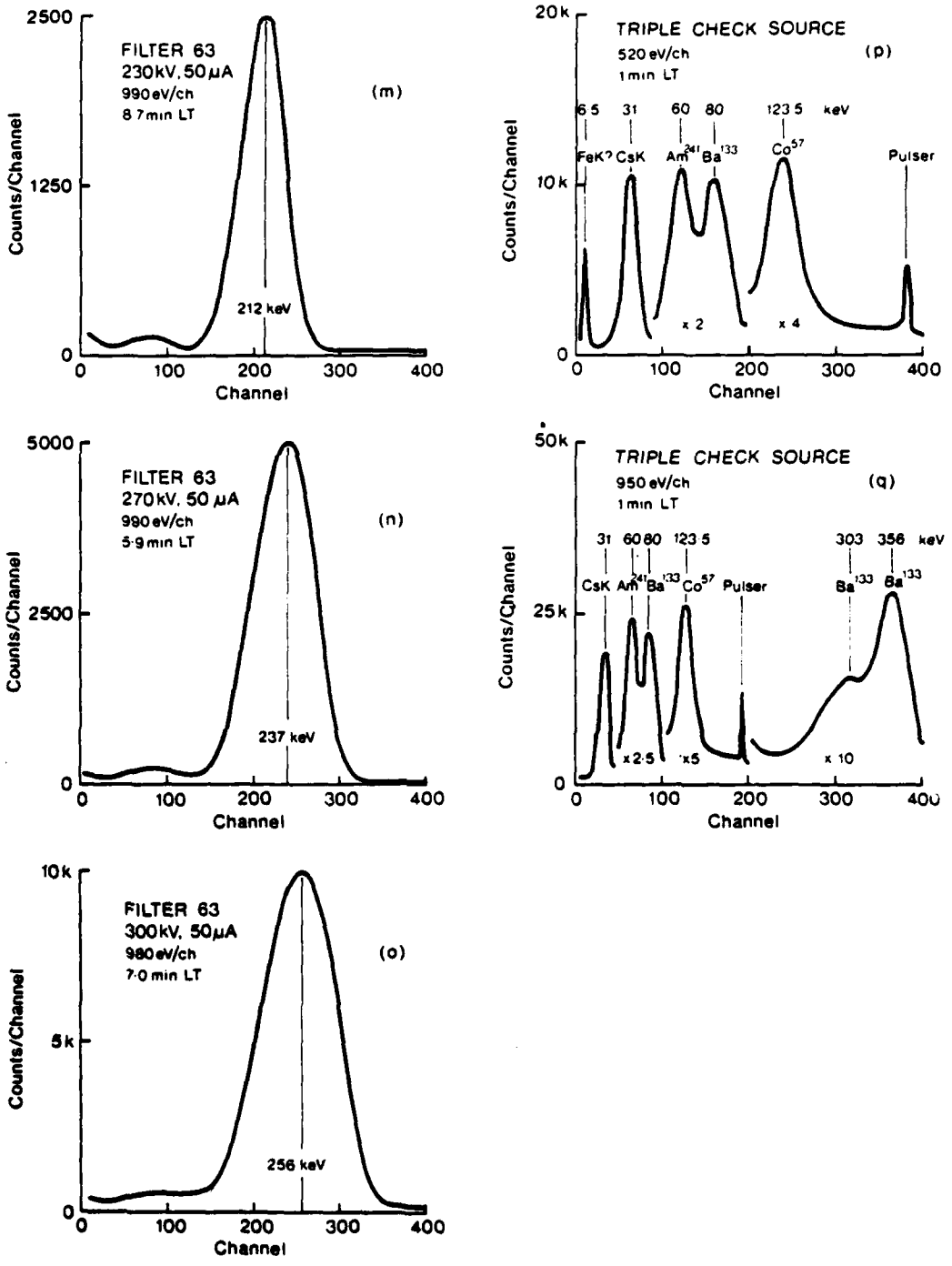

FIG. 8 - Typical main X-ray beam measured spectra and radioactive source calibration spectra
Part 3: X-ray beam examples (m) to (o) and calibration examples (p) to (q)
Data includes filter number, set kV, tube current, and multi-channel analyser sensitivity (eV/ch) and live time (LT).

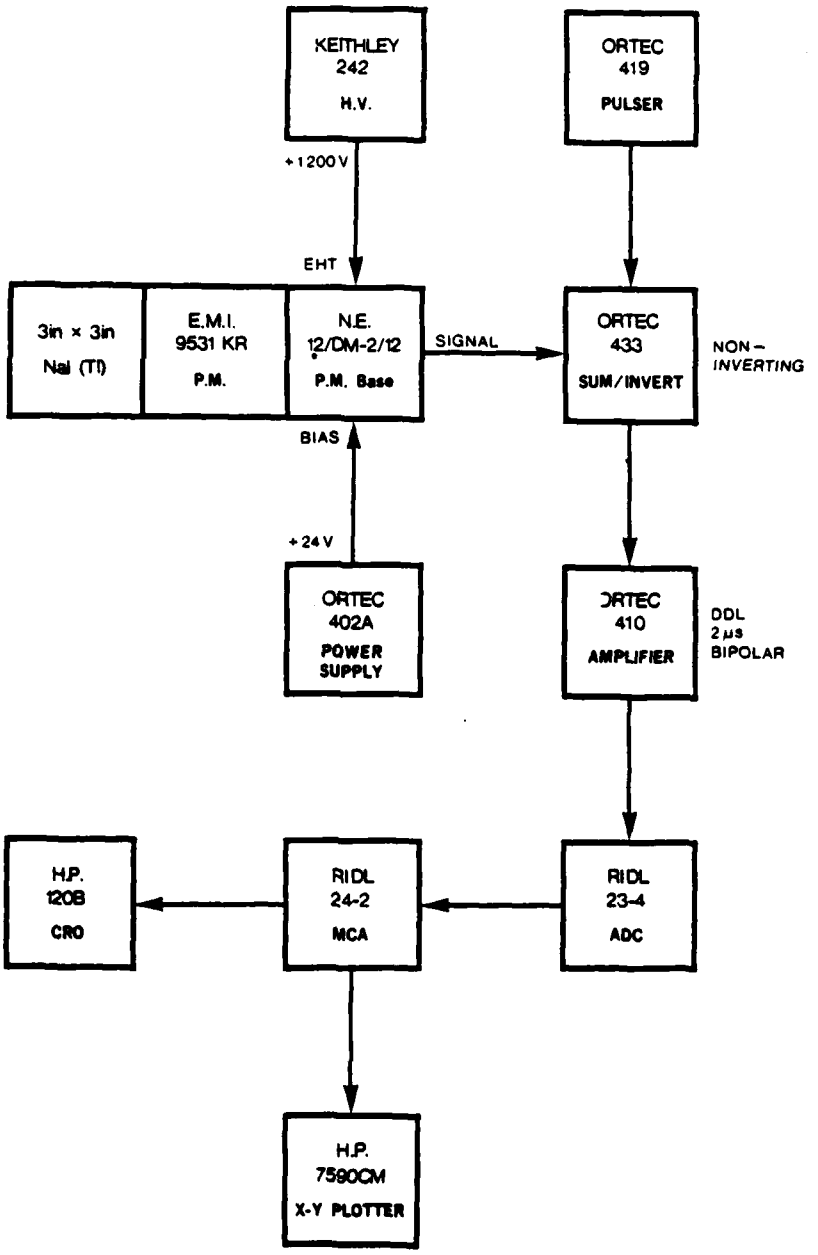

FIG. 9 - Block diagram showing NaI(T1) scintillation spectrometer and associated electronic equipment.

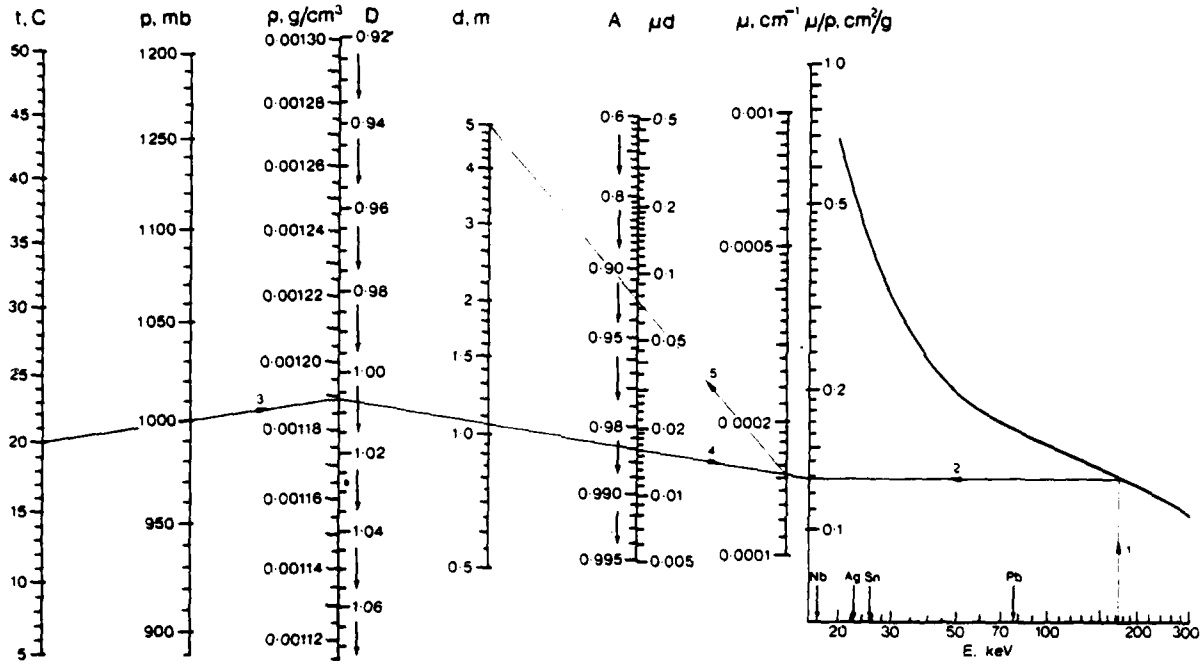

FIG. 10 - Nomograph for determination of air attenuation and air density correction factors A and D.
Example: Given a modal energy E = 173 keV, test distance d = 5m, temperature t = 20°C, and pressure p = 1000 mb, steps 1 to 5 show how the values A = 0.926 and D = 1.007 are determined.

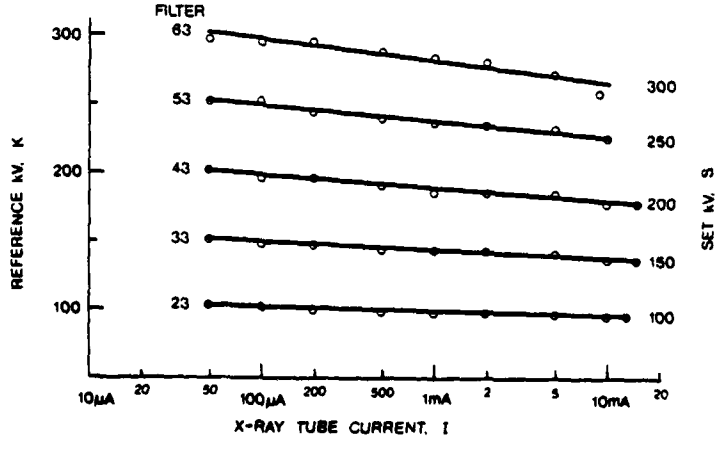

FIG. 11 - Variation of reference kV,K, with tube current I and set kV,S.

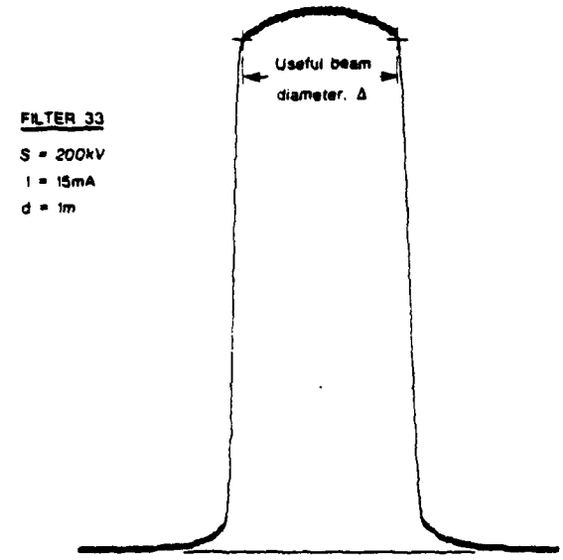

FIG. 12 - Typical X-ray beam profile scan showing the useful beam diameter Δ

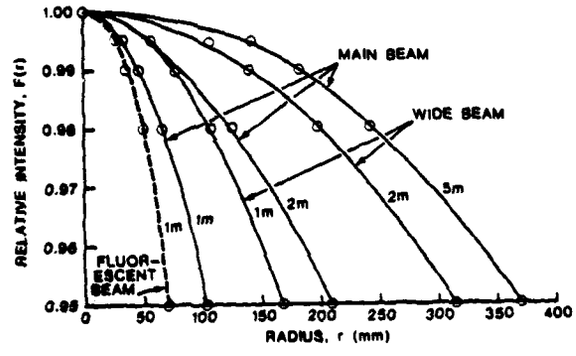

FIG. 13 - X-ray profile function F(r) for various test distances

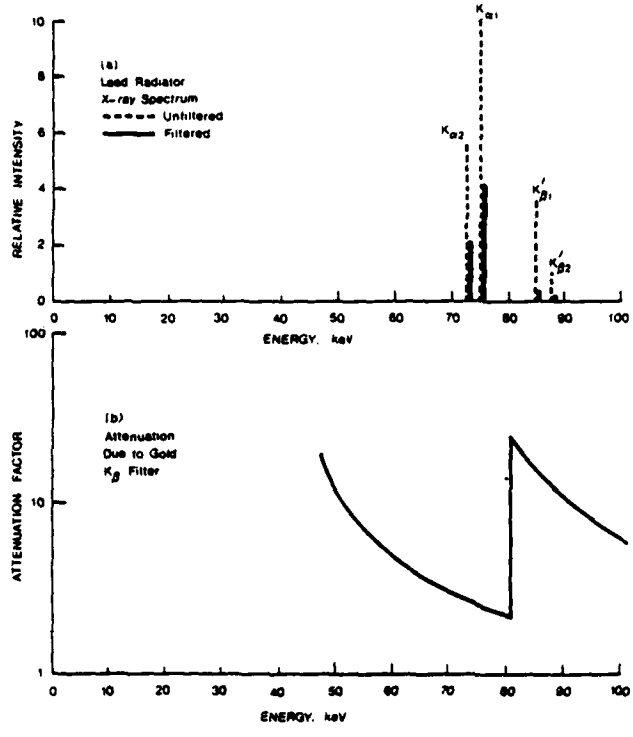

FIG. 14 - Preferential attenuation of lead K_β X-rays by a gold post-filter.

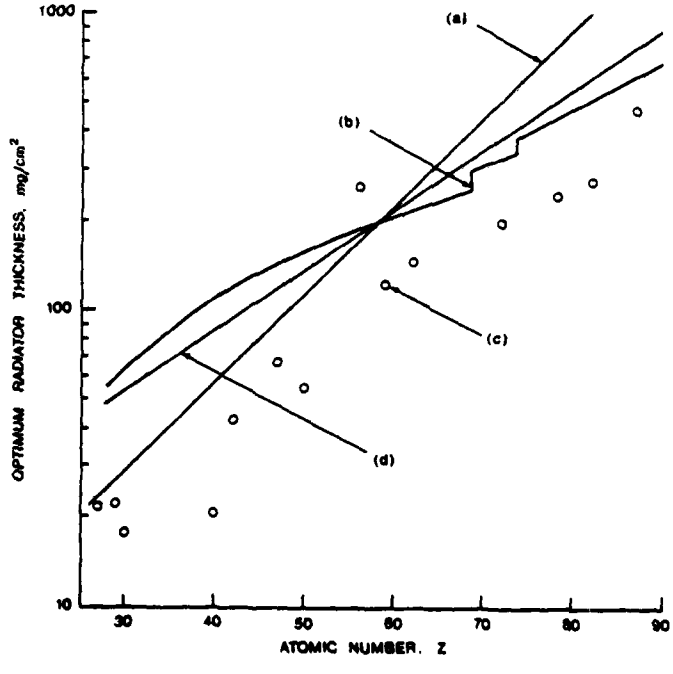

FIG. 15 - Variation of radiator foil thickness t with atomic number Z. Showing (a) the function $t = 3.6e^{0.069Z}$ given by Kathren et al [12], (b) a curve given by Storm et al [9], (c) foil thicknesses used by Ebert et al [11], and (d) the function $t = 13.5e^{0.046Z}$ used in the present work.

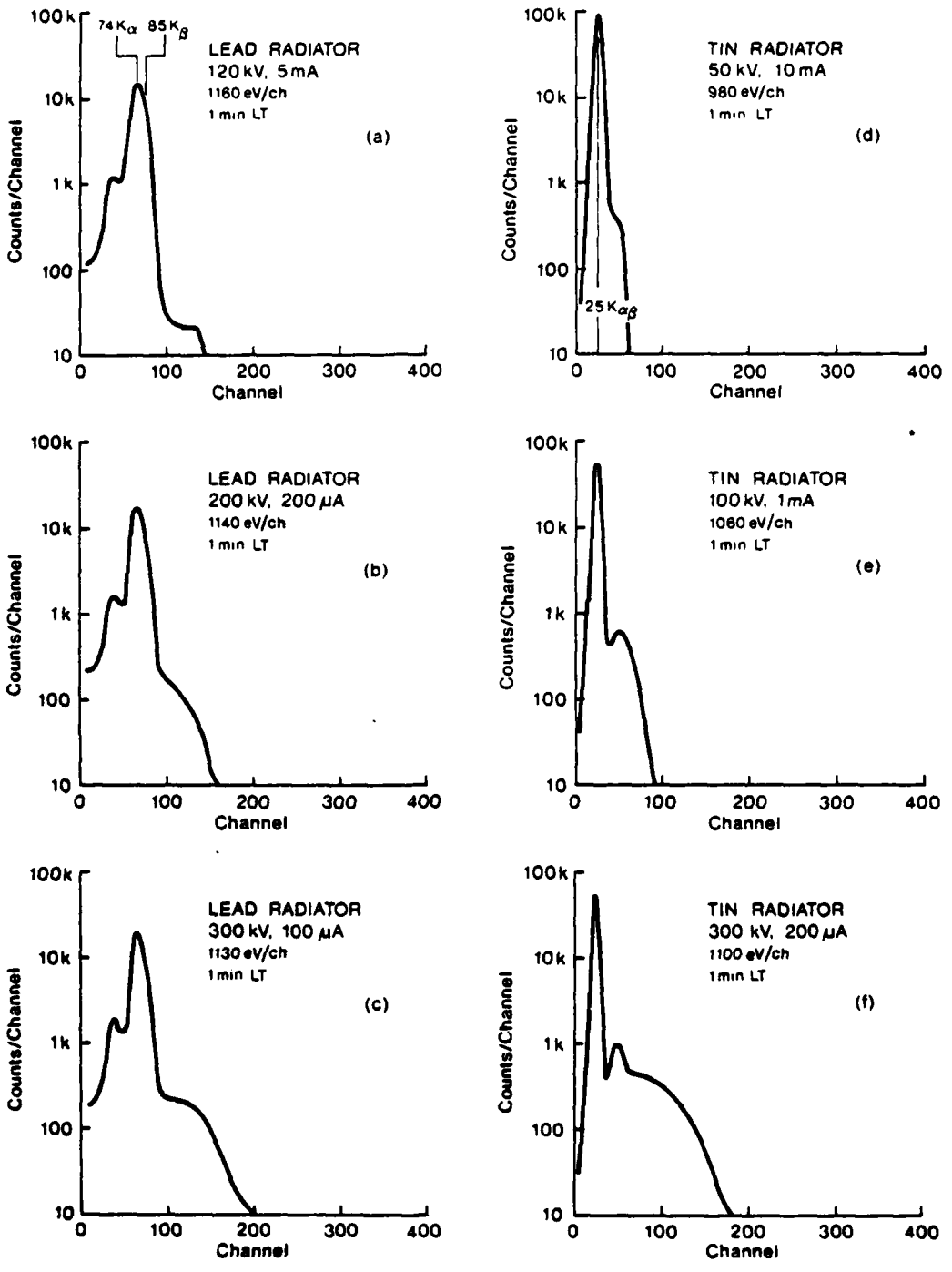

FIG. 16 - Typical fluorescent X-ray beam measured spectra and radioactive source calibration spectra

Part 1: X-ray examples (a) to (f)

Data includes radiator foil, set kV, tube current, and multi-channel analyser sensitivity (eV/ch) and live time (LT).

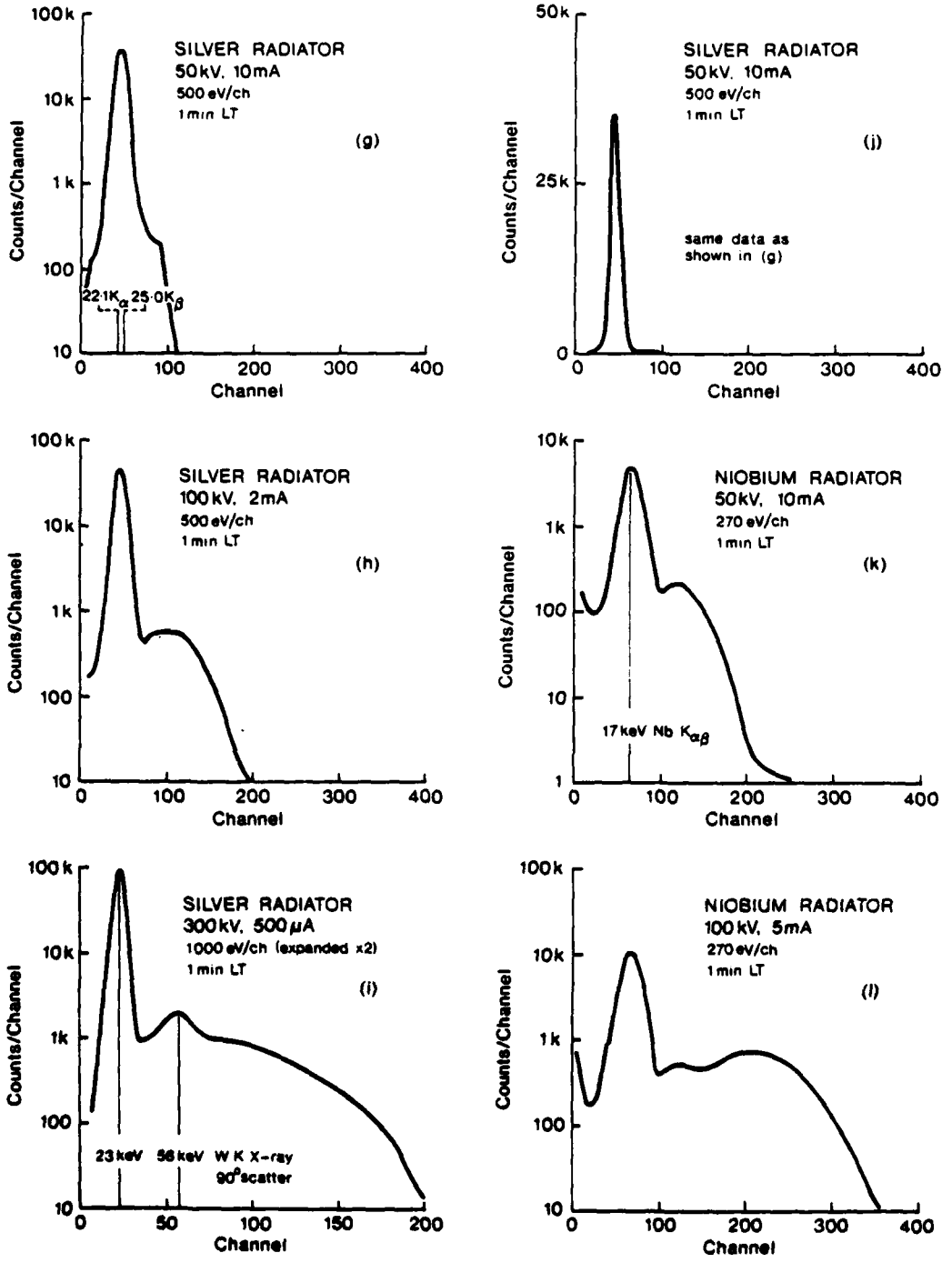

FIG. 16 - Typical fluorescent X-ray beam measured spectra and radioactive source calibration spectra

Part 2: X-ray examples (g) to (l)

Data includes radiator foil, set kV, tube current, and multi-channel analyser sensitivity (eV/ch) and live time (LT).

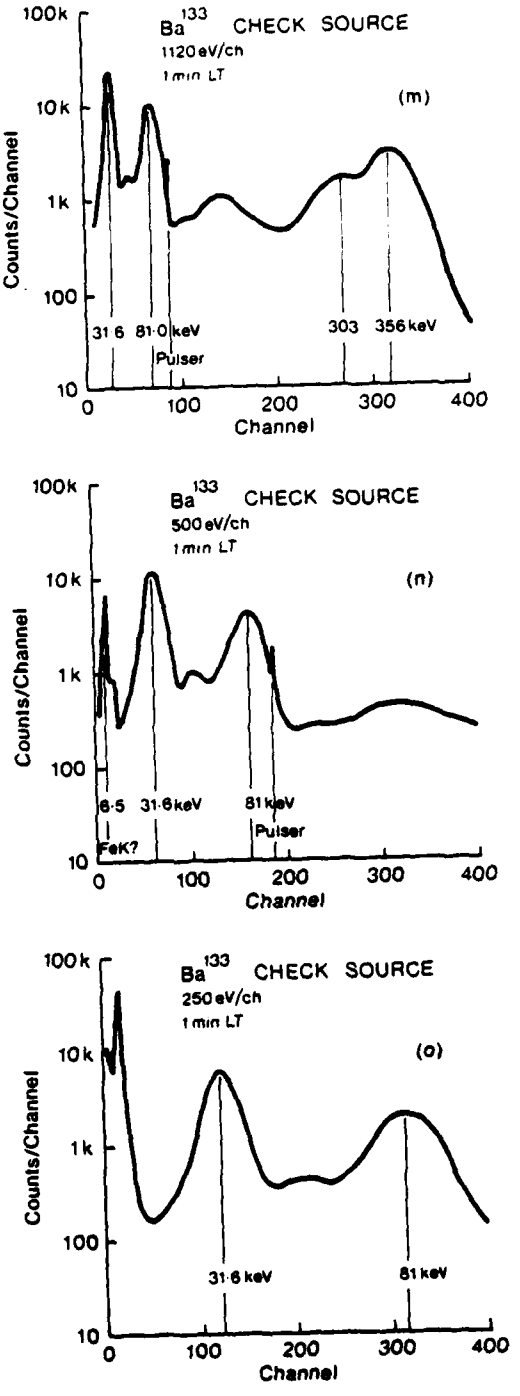

FIG. 16 - Typical fluorescent X-ray beam measured spectra and radioactive source calibration spectra

Part 3: Calibration examples (m) to (o)

Data includes radiator foil, set kV, tube current, and multi-channel analyser sensitivity (eV/ch) and live time (LT).

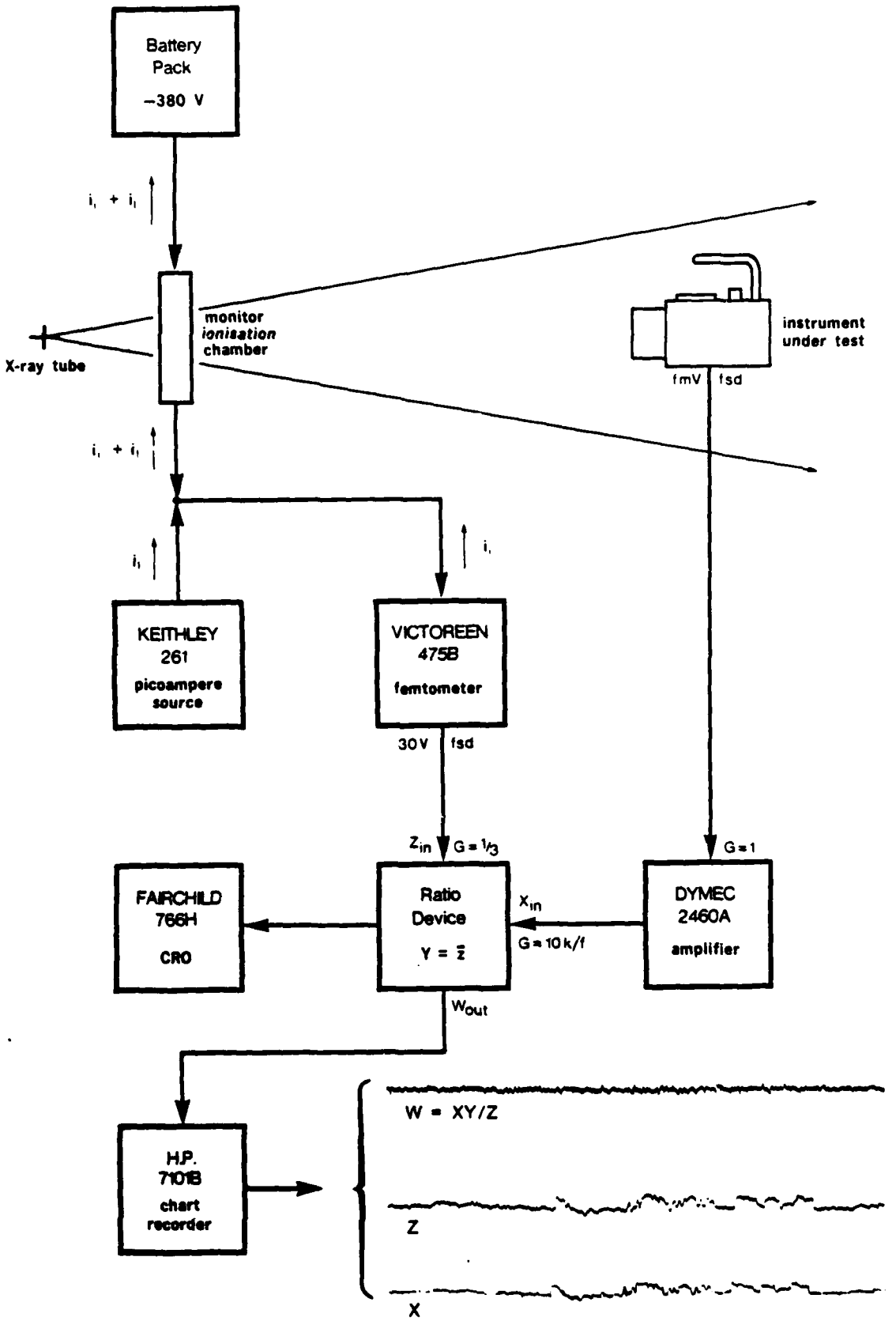

FIG. 17 - Monitor chamber and electronic ratio device measurement system as set-up for calibration of a radiation measuring instrument

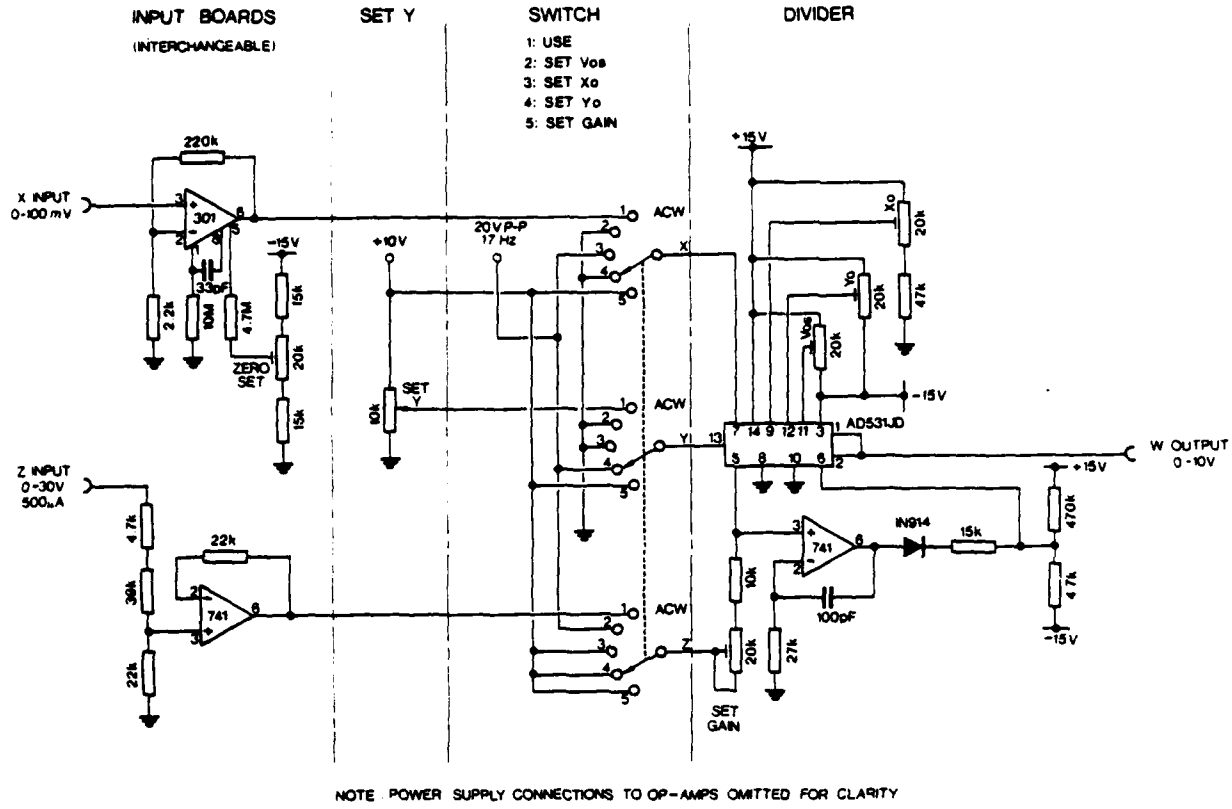

FIG. 18 - Electronic ratio device main circuit diagram

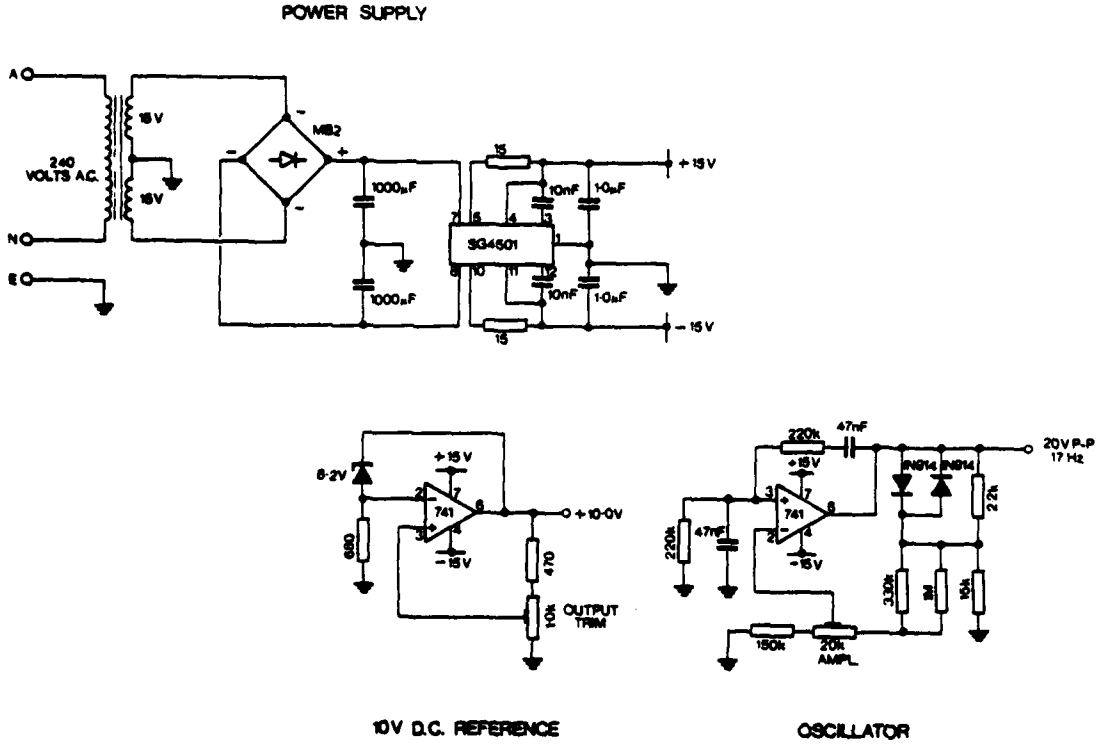

FIG. 19 - Electronic ratio device auxiliary circuit diagrams

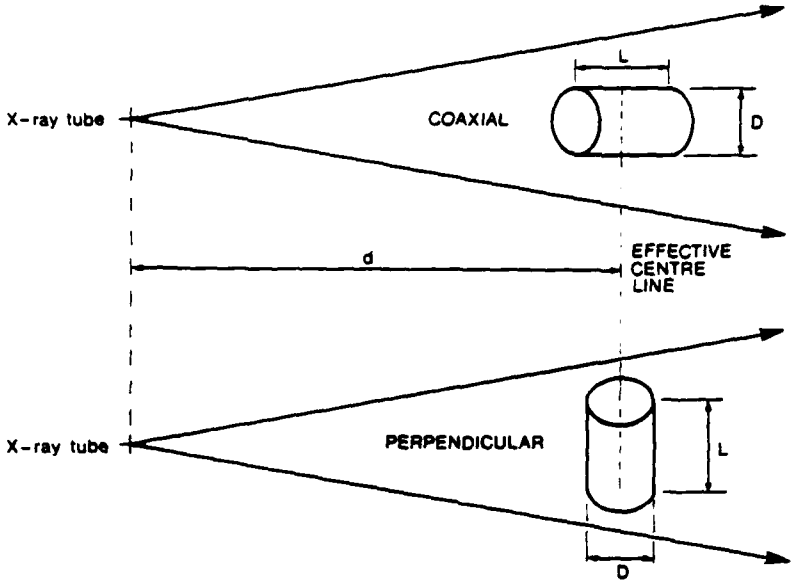

FIG. 20 - Coaxial and perpendicular modes of irradiation of a cylindrical radiation detector.

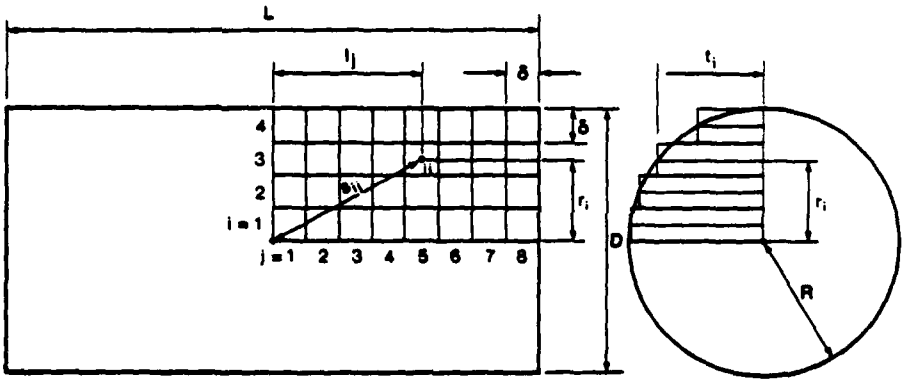

FIG. 21 - System of elements for the double summation in equation (18)

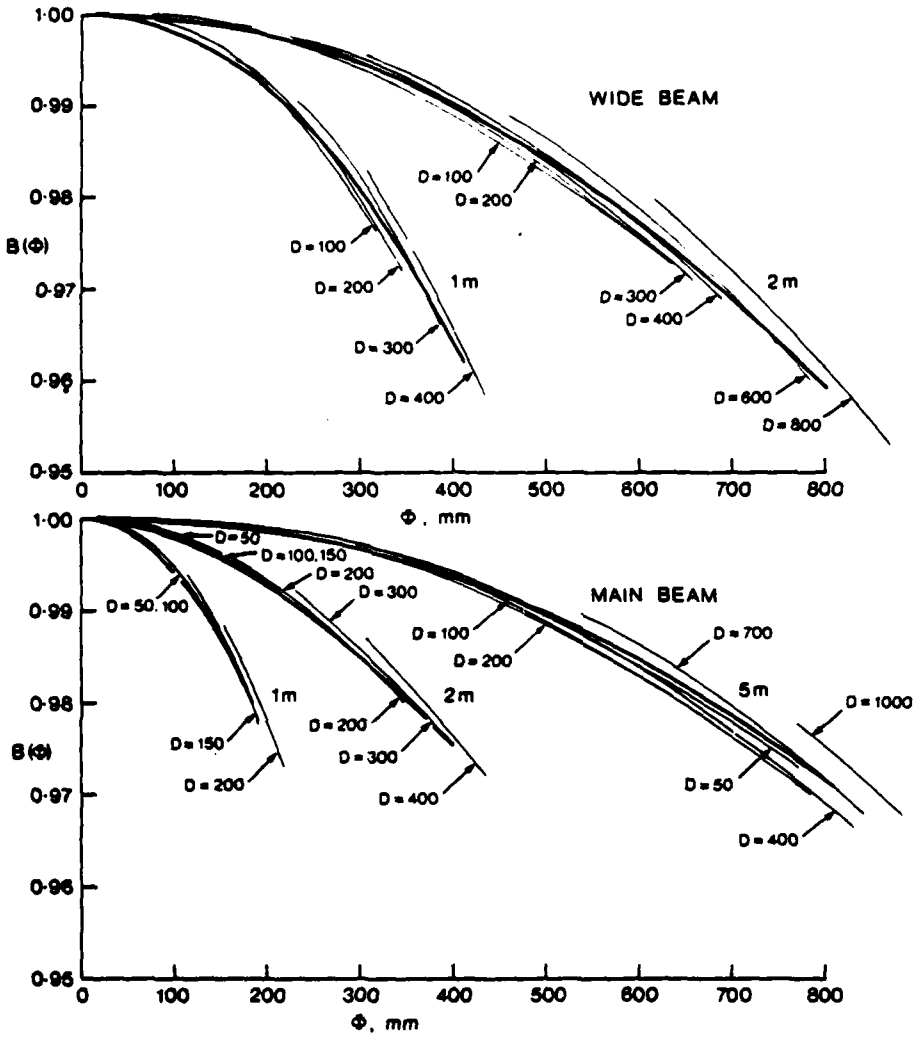

FIG. 22 - **Beam profile correction factors B (Φ) for the main and wide X-ray beams**
The thick and thin lines are respectively for coaxial and perpendicular irradiation of a cylindrical radiation detector of diameter D mm and length L mm. The equivalent coaxial diameter Φ is given by Φ = D, coaxial case, and $\Phi = \sqrt{L^2 + D^2}/1.3$, perpendicular case.

EXAMPLES ILLUSTRATING USE OF THE NOMOGRAPHS IN FIGS. 23 AND 24

Example 1:

Coaxial irradiation of a 500 mm diameter cylindrical detector at a test distance of 3 m in the main X-ray beam.

Joining the points d = 3 m and Φ = D = 500 mm in Fig. 24 gives B = 0.979 using the main beam scales for d and B. The nomograph shows also that the useful beam diameter Δ = 600 mm at the given test distance, hence it may be concluded that the detector will be fully irradiated by the beam.

Example 2:

Perpendicular irradiation of a 230 mm diameter and 290 mm long cylindrical detector at a test distance of 1 m in the wide X-ray beam.

Joining the points d = 1 m and $\Phi = \sqrt{L^2 + D^2}/1.3$ = 285 mm in Fig. 24 gives B = 0.982 using the wide beam scales. The useful beam diameter Δ = 400 mm. This will be sufficient to fully irradiate the cylinder, as the nomograph in Fig. 23 shows that the minimum beam diameter required for this purpose is Δ_c = 370 mm. Fig. 23 also indicates the value Φ = 285 mm calculated above.

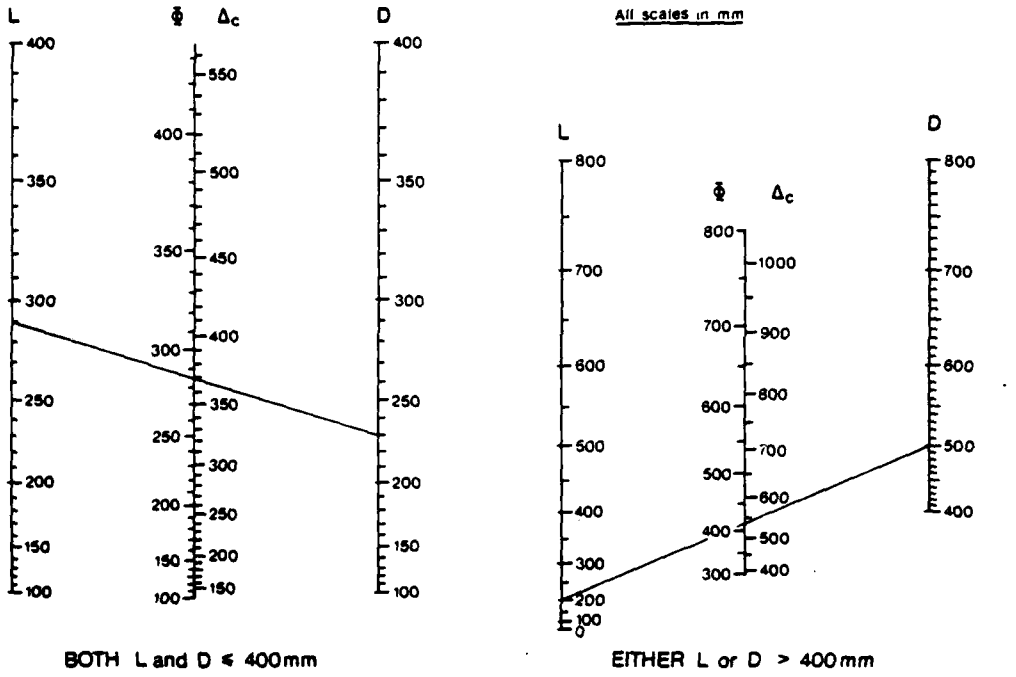

FIG. 23 - Monograph for determination of the equivalent coaxial diameter Φ of a cylindrical radiation detector irradiated perpendicularly, and the corresponding minimum beam width Δ_c.

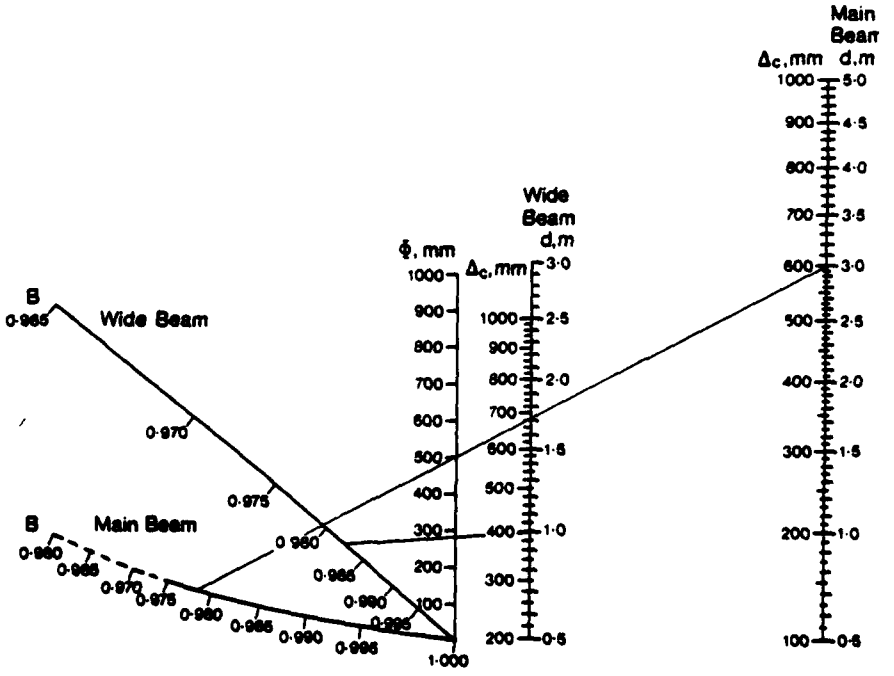

FIG. 24 - Nomograph for determination of the beam profile correction factor $B(\Phi)$ for a cylindrical radiation detector irradiated coaxially or perpendicularly.

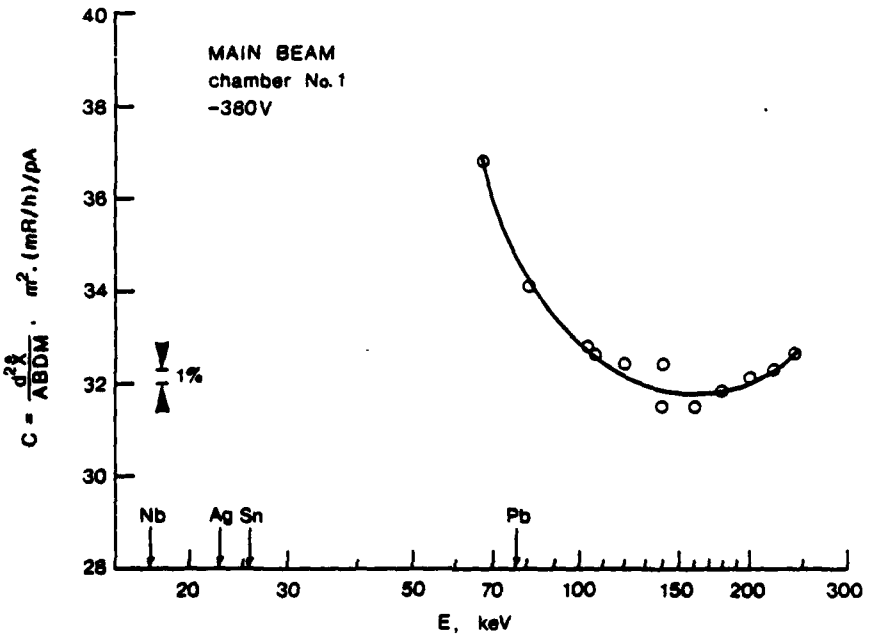

FIG. 25 - Variation of the monitor chamber calibration factor C with modal energy E of the main X-ray beam

(MRL-R-910)

DISTRIBUTION LIST

MATERIALS RESEARCH LABORATORIES

DIRECTOR
Superintendent, Physics Division
Dr D.W. Williams
Mr J.W. Allison
Library (2 copies)
Mr R.B. Huntley (20 copies)

DEPARTMENT OF DEFENCE

Chief Defence Scientist (for CDS/DCDS/CPAS/CERPAS) (1 copy)
Army Scientific Adviser
Air Force Scientific Adviser
Navy Scientific Adviser
Officer-in-Charge, Document Exchange Centre (17 copies)
Technical Reports Centre, Defence Central Library
Central Office, Directorate of Quality Assurance - Air Force
Deputy Director Scientific, and Technical Intelligence, Joint Intelligence Organisation.
Librarian, Bridges Library
Librarian, Engineering Development Establishment
Defence Science Representative, (Summary Sheets Only)
Australia High Commission, London.
Counsellor Defence Science, Washington D.C. (Summary Sheets Only)
Librarian, (Through Officer-in-Charge), Materials Testing Laboratories, ALEXANDRIA, N.S.W.
Senior Librarian, Aeronautical Research Laboratories
Senior Librarian, Defence Research Centre Salisbury, S.A.

DEPARTMENT OF DEFENCE SUPPORT

Deputy Secretary, DDS
Head of Staff, British Defence Research & Supply Staff (Aust.)

OTHER FEDERAL AND STATE DEPARTMENTS AND INSTRUMENTALITIES

NASA Canberra Office, Woden, A.C.T.
The Chief Librarian, Central Library, C.S.I.R.O.
Library, Australian Atomic Energy Commission Research Establishment

DISTRIBUTION LIST

(Continued)

MISCELLANEOUS - AUSTRALIA

Librarian, State Library of NSW, Sydney, NSW
University of Tasmania, Morris Miller Library, Hobart, TAS.
Director, Australian Radiation Laboratory, Yallambie, VIC.
Librarian, Australian Radiation Laboratory, Yallambie, VIC. (2 copies)
Mr N. Hargrave, Australian Radiation Laboratory, Yallambie, VIC.
Mr E. Heywood, Royal Melbourne Institute of Technology, Melbourne, VIC.

MISCELLANEOUS - OVERSEAS

Library - Exchange Desk, National Bureau of Standards, U.S.A.
UK/USA/CAN/NZ ABCA Armies Standardisation Representative (4 copies)
Director, Defence Research Centre, Kuala Lumpur, Malaysia
Exchange Section, British Library, U.K.
Periodicals Recording Section, Science Reference Library, British Library, U.K.
Library, Chemical Abstracts Service
INSPEC: Acquisition Section, Institute of Electrical Engineers, U.K.
Engineering Societies Library, U.S.A.
Aeromedical Library, Brooks Air Force Base, Texas, U.S.A.
Ann Germany Documents Librarian, The Centre for Research Libraries, Chicago I11.
Defense Attache, Australian Embassy, Bangkok, Thailand Att. D. Pender